

# GAIA: A Global, Multi-modal, Multi-scale Vision-Language Dataset for Remote Sensing Image Analysis

Angelos Zavras, Dimitrios Michail, Xiao Xiang Zhu *Fellow Member, IEEE*, Begüm Demir *Senior Member, IEEE*, Ioannis Papoutsis

**Abstract**—The continuous operation of Earth-orbiting satellites generates vast and ever-growing archives of Remote Sensing (RS) images. Natural language presents an intuitive interface for accessing, querying, and interpreting the data from such archives. However, existing Vision-Language Models (VLMs) are predominantly trained on web-scraped, noisy image-text data, exhibiting limited exposure to the specialized domain of RS. This deficiency results in poor performance on RS-specific tasks, as commonly used datasets often lack detailed, scientifically accurate textual descriptions and instead emphasize solely on attributes like date and location. To bridge this critical gap, we introduce GAIA, a novel dataset designed for multi-scale, multi-sensor, and multi-modal RS image analysis. GAIA comprises of 205,150 meticulously curated RS image-text pairs, representing a diverse range of RS modalities associated to different spatial resolutions. Unlike existing vision-language datasets in RS, GAIA specifically focuses on capturing a diverse range of RS applications, providing unique information about environmental changes, natural disasters, and various other dynamic phenomena. The dataset provides a spatially and temporally balanced distribution, spanning across the globe, covering the last 25 years with a balanced temporal distribution of observations. GAIA’s construction involved a two-stage process: (1) targeted web-scraping of images and accompanying text from reputable RS-related sources, and (2) generation of five high-quality, scientifically grounded synthetic captions for each image using carefully crafted prompts that leverage the advanced vision-language capabilities of GPT-4o. We also release an automated processing framework developed for this purpose, enabling the broader research community to generate captions for RS images using the web-crawled image-text data. Our extensive experiments, including fine-tuning of CLIP and BLIP2 models, demonstrate that GAIA significantly improves performance on RS image classification, cross-modal retrieval and image captioning tasks, proving its value as a crucial resource for advancing the field.

**Index Terms**—Vision-language dataset, vision-language model,

Angelos Zavras is with the Orion Lab, School of Rural, Surveying and Geoinformatics Engineering, National Technical University of Athens, 15772 Athens, Greece & Institute of Astronomy, Astrophysics, Space Applications and Remote Sensing, National Observatory of Athens, 11810 Athens, Greece, and with the Department of Informatics and Telematics, Harokopio University of Athens, 17676 Athens, Greece (e-mail: azavras@noa.gr).

Dimitrios Michail is with the Department of Informatics and Telematics, Harokopio University of Athens, 17676 Athens, Greece (e-mail: michail@hua.gr).

Xiao Xiang Zhu is with the Chair of Data Science in Earth Observation, Technical University of Munich, 80333 Munich, Germany, and also with the Munich Center for Machine Learning, 80333 Munich, Germany (e-mail: xiaoxiang.zhu@tum.de).

Begüm Demir is with the Faculty of Electrical Engineering and Computer Science, Technische Universität Berlin, 10623 Berlin, Germany, also with the BIFOLD - Berlin Institute for the Foundations of Learning and Data, 10623 Berlin, Germany (e-mail: demir@tu-berlin.de).

Ioannis Papoutsis is with the Orion Lab, School of Rural, Surveying and Geoinformatics Engineering, National Technical University of Athens, 15772 Athens, Greece & Institute of Astronomy, Astrophysics, Space Applications and Remote Sensing, National Observatory of Athens, 11810 Athens, Greece (e-mail: ipapoutsis@mail.ntua.gr).

representation learning, remote sensing.

## I. INTRODUCTION

THE Earth’s orbit is teeming with a growing constellation of Earth Observation (EO) satellites, continuously producing an unprecedented volume of diverse and complex information about our planet. According to the latest Copernicus Sentinel Data Access Annual Report <sup>1</sup>, Europe’s Copernicus satellite constellation alone features an average daily publication rate of more than 20 TiB of user-level data. More specifically, within the reporting period from January 1, 2023 to October 31, 2023, a total of more than 11.5 million user-level data were published, accounting for a total data volume of 6.04 PiB. To put this into perspective, the 6.04 PiB published during the aforementioned reporting period alone is more than ESA’s entire collection of EO data from the pre-Copernicus era, which amounted to 5.6 PB at the end of 2013. It is evident that this exponential growth in data production has outpaced our capacity for meaningful information extraction, prompting the Remote Sensing (RS) community to adopt Deep Learning (DL) approaches to extract meaningful insights for Earth observation.

In this data-rich landscape [1], language provides a natural interface to interact with and analyze these vast RS archives. Language provides a compressed representation of reality, efficiently encoding concepts. However, this compression is lossy and language alone lacks vital knowledge of the physical world that can only be acquired through sensory experience. To this end, Vision-Language models (VLMs) offer a solution by leveraging the richness of visual (image) data alongside the compression of textual information. By combining these modalities, VLMs are able to learn abstract representations that encapsulate comprehensive scene understanding. VLMs hold immense potential for the RS domain. By comprehending concepts from both visual and language modalities, VLMs can enable intuitive interfaces for RS data analysis (e.g. image captioning, cross-modal retrieval and visual question answering) or even serve as versatile building blocks for next-generation of RS foundation models.

Data is regarded as the cornerstone for VLM training in the computer vision domain, a principle firmly established in the foundation models literature [2], and the RS domain is no exception. Existing general purpose VLMs are trained on large amounts of web-crawled data, to encode general knowledge, without emphasizing on specialized domains such as RS and

<sup>1</sup><https://sentinels.copernicus.eu/web/sentinel/-/ninth-copernicus-sentinel-data-access-annual-report>

medical imagery, which as a matter of fact demonstrate fundamentally different distributions compared to natural images encountered during pre-training. Perhaps most critically, unlike natural image-text datasets, which can easily reach billion-scale [3], [4], specialized datasets hold a relatively limited scale due to their innate demand for highly targeted knowledge and substantial human labor, rendering it costly and often impractical.

The advancements in Vision-Language Models (VLMs) have drawn significant attention in the RS field, leading to studies across different applications. While early attempts have shown the potential of applying VLMs to RS, it is still an emerging field with many unsolved challenges [5]. A challenging issue that impedes the development of VLMs in RS is the lack of large-scale aligned image-text datasets. Existing RSI datasets mostly focus on visual recognition tasks and do not provide language annotations. While there have been some efforts to create RS image-text paired datasets, their scale, quality, and diversity still leave room for improvement.

Recent initiatives such as LAION-EO [6] have demonstrated the presence of RS-related samples within large-scale web-crawled image-text paired datasets like LAION-5B [3]. However, these samples frequently lack the depth and specificity needed for domain-specific RS applications. They primarily focus on or are limited to basic attributes such as date and location, neglecting critical RS-specific semantic information including land cover types, geospatial context, and environmental features. This limits the applicability of these datasets for developing high-quality RS image analysis models, which require precise and context-rich in-domain annotations.

Existing datasets for training VLMs in the RS domain suffer from significant limitations that hinder the development of effective in-domain models or the adaptation of existing pre-trained VLMs to RS tasks. To begin with, the predominant reliance on aerial and Very High-Resolution (VHR) commercial satellite imagery in widely used, yet limited-scale, datasets [7]–[10] introduces two primary challenges. First, the proprietary nature of this data restricts accessibility and reproducibility, contrasting with the open-access paradigm promoted by missions like the Copernicus Sentinel. Second, the finer spatial resolution inherent in these datasets, while advantageous for specific applications, creates a domain shift compared to data from non-commercial, often coarser-resolution satellite missions. On the other hand, more recent works exploit existing class-labeled datasets in order to automatically generate synthetic captions reaching up to million-scale capacity. Despite addressing the dataset scale aspect, these methods, similar to existing manually curated datasets, fail to adequately support the development of robust in-domain VLMs capable of generalizing across the diverse landscape of RS applications and data sources, due to their severely limited level of caption detail and lack of diverse, domain-specific vocabulary.

To address these challenges, we release GAIA, a dataset of approximately 41,030 RS images, each accompanied by five diverse and informative captions, resulting in 205,150 image-text pairs. Specifically, less than 3% of GAIA’s images are found in compared web-crawled datasets. Moreover, we

provide extensive benchmarks for RS image classification and cross-modal retrieval tasks by fine-tuning CLIP on the GAIA dataset, and we publish the pre-trained model weights to facilitate further research. Complementing the dataset, we introduce a novel automated processing framework for generating RS image descriptions by leveraging web-crawled data from reputable sources and the advanced language generation capabilities of ChatGPT. Our work aims to bridge the gap between the vast potential of VLMs and the unique challenges of the RS domain, accelerating the development of foundation models that can unlock new insights from Earth observation data. We make our dataset, automated processing framework and fine-tuned model weights publicly available on our project’s GitHub repository<sup>2</sup>.

Our main contributions can be summarized as follows:

- 1) We introduce GAIA, a carefully curated RS dataset with 41,030 images along 5 synthetic captions each (205,150 image-text pairs) featuring global, multi-modal, multi-scale coverage spanning across the last 25 years. It exhibits minimal overlap (< 3%) with existing datasets, enabling diverse Earth event analysis across multiple spatial resolutions and modalities.
- 2) We release a novel, automated processing framework for generating detailed and scientifically grounded textual descriptions and rich metadata for RS imagery. Our framework leverages targeted web-scraped data from reputable RS websites and harnesses the advanced vision-language capabilities of GPT-4o to produce five high-quality captions per image, significantly enriching the semantic content compared to original alt-text.
- 3) We evaluate GAIA’s impact extensively by fine-tuning CLIP and BLIP2 models on both alt-text and synthetic captions for RS scene classification, cross-modal retrieval, and image captioning. Our benchmarking demonstrates substantial performance improvements, with synthetic captions proving superior in enhancing semantic alignment and task accuracy. We release pre-trained models to facilitate future RS VLM-related research.

## II. RELATED WORK

Vision-Language Models (VLMs) have emerged as powerful tools for understanding and generating connections between visual and textual information. Pioneering works like CLIP [11] demonstrated the effectiveness of contrastive learning in creating aligned visual-semantic embeddings, while more recent models such as LLaVA [12], [13] have expanded these capabilities to include sophisticated visual reasoning and open-ended dialogue. Modern VLMs can perform a wide range of tasks, including image captioning, visual question answering, and cross-modal retrieval without task-specific fine-tuning. The success of these models stems from their ability to learn generalizable visual-semantic representations through self-supervised learning on vast amounts of image-text data, typically utilizing web-scale datasets containing billions of image-text pairs. This approach has proven particularly

<sup>2</sup><https://github.com/Orion-AI-Lab/GAIA>

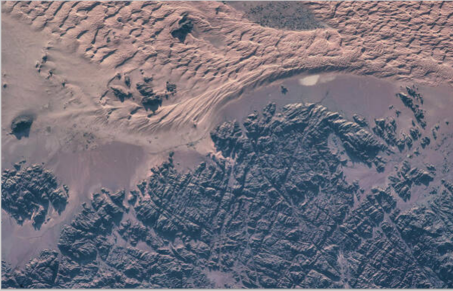
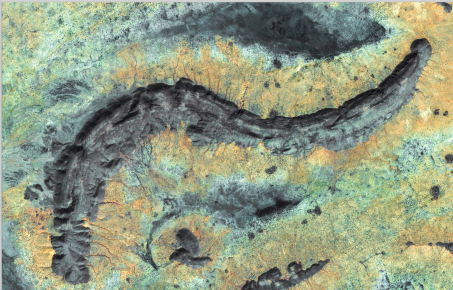
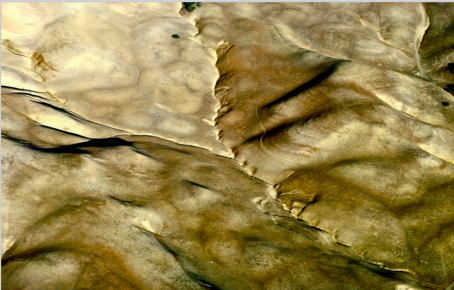
LAION-EO Dataset Samples		
exmouth australia google earth fractals Fractal Patterns in Nature Found on Google Earth	Peruvian Andes. © Contains modified Copernicus Sentinel data (2020), processed by ESA, CC BY-SA 3.0	Iss Photograph - Satellite View Of Wet Sand On Riverbed by Panoramic Images
		
google-earth-Niger-Magaria-13708	Aerial Photo	Lake_powell_utah-from-space.jpg
		

Fig. 1. Representative samples from the LAION-EO [6] dataset illustrate a fundamental limitation inherent in web-scraped image-text paired datasets for remote sensing: despite images exhibit sufficient visual fidelity, the accompanying textual descriptions are characterized by high noise levels and lack domain-specific details, diminishing their utility for Earth Observation tasks.

effective at capturing nuanced relationships between visual content and natural language descriptions, enabling zero-shot transfer to novel tasks and domains.

#### A. Have existing VLMs seen Remote Sensing imagery?

While VLMs excel at general visual and textual understanding, their training on massive, web-scraped datasets like LAION-5B raises concerns about their proficiency in specialized domains such as RS [14]. Recent studies employing rigorous filtering techniques on these large-scale datasets have provided compelling evidence that VLMs have indeed encountered RS images, but this exposure is incidental, unsystematic, and ultimately superficial. This limited and unfocused engagement with RS data highlights a crucial gap in the capabilities of current VLMs.

Several research efforts have focused on extracting RS subsets from web-crawled large-scale general-purpose datasets, extensively used within the computer vision domain. As an example, Czerkawski and Francis developed LAION-EO [6], leveraging CloudSEN12 [15] as an "anchor dataset" of Sentinel-2 images to retrieve similar images from LAION-5B. Their multi-stage filtering process, involving nearest neighbor search and refined CLIP-based similarity thresholds, yielded 24k samples in the prototype version and an expanded set of 113k in version 1. Similarly, Zhang et al. [16] identified LAION-RS, a subset of 726k RS images, i.e. a mere 0.03% of LAION-2B, using a binary classifier. Zhang et al. [17] introduced RS5M, a dataset of 5 million RS image-text pairs. A core component of RS5M, the PUB11 subset containing over 3 million pairs, was created by filter-

ing 11 large-scale public datasets using keyword-based filtering, de-duplication, and a VLM-based filter. The 11 filtered large-scale public datasets, include LAION2B-en [3], LAION400M [18], LAIONCOCO [19], COYO700M [20], CC3M [21], CC12M [22], YFCC15M [23], WIT [24], Redcaps [25], SBU [26], and Visual Genome [27]. These filtering efforts offer critical insights into the current state of VLMs. First, the relatively small size of the extracted subsets, such as the minuscule 0.03% of LAION-2B forming LAION-RS, demonstrates the limited and incidental exposure of VLMs to RS data. Second, as shown in Fig. 1, web-scraped datasets like LAION-EO present a significant challenge: while the extracted imagery is generally of sufficient quality and resolution, the associated captions are inadequate for RS image analysis. They are dominated by generic attributes and lack the detailed, domain-specific descriptions, thus fail to describe land cover types, specific geographical features, or other essential elements that are crucial in RS downstream tasks.

These findings demonstrate that the current generation of VLMs, trained on vast yet generic datasets, possesses an inadequate representation of the RS domain, resulting in shallow and insufficient understanding of RS imagery. Their incidental and unsystematic exposure has resulted in a limited ability to capture the rich semantic details and domain-specific knowledge required for effective RS image analysis. Therefore, the development of dedicated high-quality RS image-text datasets, coupled with specialized model architectures, plays a pivotal role in advancing the field, paving the way for more sophisticated and impactful applications.

## B. Remote Sensing Image-Text Paired Datasets

The increasing availability of RS images, coupled with the remarkable advancements in deep learning (DL), have generated unprecedented opportunities for automated satellite scene understanding, object detection, and change analysis at a global scale. However, the success of these data-intensive DL models hinges critically on the existence of large-scale, high-quality training datasets. While the computer vision community has witnessed the creation of massive image-text paired datasets like LAION-5B, the RS domain lags behind, primarily due to the inherent complexities and unique challenges associated with annotating RS imagery. Creating such datasets for RS applications (see Table I) is a formidable task, requiring domain expertise, meticulous manual effort, and substantial resources to accurately describe the complex spatial relationships, diverse land cover types, and varying scales present in aerial and satellite imagery.

Early efforts in associating RS imagery with textual descriptions were pioneered by [7] introducing two novel datasets towards semantic understanding of high-resolution RS images: the UCM-Captions dataset and the Sydney-Captions dataset. The UCM-Captions dataset, derived from the UC Merced Land Use dataset [28], contains 2,100 aerial images with spatial resolution of 0.3m across 21 land-use classes, sourced from the USGS National Map Urban Area Imagery. The Sydney-Captions dataset features 613 images with spatial resolution of 0.5m across 7 land-use classes, sourced from a Google Earth. Both datasets contain five manually crafted captions for each image, describing the scene’s semantic content, including objects, attributes, and their relationships. However, while the captions for each image vary in phrasing, descriptions for images within the same class show limited diversity, often focusing on similar aspects and sentence structures, revealing a limitation in capturing the diverse perspectives of human observers.

Building upon the aforementioned foundational datasets, Lu et al. [8] introduced the RSICD dataset, significantly expanding the scale and scope of RS image-text paired datasets available at the time. RSICD contains 10,921 aerial images featuring varying spatial resolutions, collected from multiple sources including Google Earth, Baidu Map, MapABC, and Tianditu, with the objective of achieving high intra-class variance and low inter-class similarity. The images were initially annotated with 24,333 descriptive sentences, with captions per image varying from 1 to 5 and subsequently extended them to 54,605 sentences by duplicating randomly the existing sentences when there are not five different sentences to describe the same image. While RSICD represented a significant advancement in terms of size and diversity compared to UCM-Captions and Sydney-Captions, it still relied on manual annotation, which limited its scalability and required substantial human effort.

To address the need for fine-grained understanding of RS imagery, Yuan et al. [9] developed the RSITMD (Remote Sensing Image-Text Match) dataset specifically designed for cross-modal RS image retrieval. RSITMD comprises of 4,743 images across 32 categories, sourced from the RSICD dataset and Google Earth. Uniquely, RSITMD emphasizes fine-grained

relationships between image attributes. Multiple annotators provided five descriptive captions per image, following guidelines to document these fine-grained relationships, alongside one to five supplementary object-level keywords. Authors demonstrated that RSITMD’s captions are more diverse than previous datasets, with a diversity score of 4.60, significantly higher than Sydney (1.83), UCM (0.97), and RSICD (1.67), capturing nuanced relationships between objects within images.

Further expanding the scale and diversity of RS image captioning datasets, the NWPU-Captions dataset, introduced by Lu et al. [29], became the largest dataset for this task at the time. It contains 31,500 images with spatial resolution ranging from 30 to 0.2 meters, covering 45 classes based on the NWPU-RESISC45 dataset [30]. Each image was manually annotated with five descriptive captions by experienced RS experts, summing up to 157,500 image-caption pairs.

The TextRS dataset, introduced by Abdullah et al. [31], focused on text-to-image matching tasks within the RS domain. TextRS contains approximately 2,144 images, each associated with five descriptive sentences summing up to 10,720 image-caption pairs. The images were randomly selected from four well-established scene classification datasets: AID [32], UC Merced [28], PatternNet [33], and NWPU [29], covering in total 134 overlapping categories. The annotation process involved five individuals generating descriptive sentences for each image, following specific guidelines to ensure diversity, accuracy, and relevance. While TextRS addressed limitations of previous datasets by incorporating diverse imagery, its reliance on manual annotation highlighted the ongoing need for automated or semi-automated approaches.

The RSVGD dataset, introduced by Li et al. [10], attempted to address the annotation bottleneck by proposing an automatic image-query generation method, although it still required manual verification to ensure correctness. The dataset was sampled from the DIOR [34] dataset, originally designed for object detection, featuring 20 object categories. Authors annotation pipeline comprised of four steps: (1) box sampling, (2) attribute extraction, (3) expression generation, and (4) manual verification. The constructed dataset contains 17,402 RS images with spatial resolution ranging from 0.5m to 30m and 38,320 image-caption pairs, where each object instance in the RS image corresponds to a unique caption. The average caption length is 7.47 words and the vocabulary size is 100 words.

Bountos et al. [35] introduced Hephaestus, a dataset designed for InSAR image analysis, offering a rich collection of manually annotated Sentinel-1 interferograms specifically designed for diverse computer vision tasks, including image captioning. The dataset has been manually annotated by a team of InSAR experts and contains 19,919 individual interferograms over 44 volcanoes across the globe, with each interferogram paired with a single, yet detailed caption. These captions provide comprehensive textual descriptions of each interferogram, including observed ground deformation, atmospheric contributions, and overall image quality. The InSAR images were acquired from the Comet-LiCS [36] portal, an automated system that processes Sentinel-1 data to generate

interferograms.

Marking a significant leap towards fully automated image-caption dataset creation, the RSTeller dataset [37], provided approximately 1.2 million image patches, each paired with multiple captions, resulting in more than 2.5 million RS image-text pairs, with a ground sampling distance of 0.6 meters. The imagery was sourced exclusively from the National Agriculture Imagery Program (NAIP) via the Google Earth Engine platform. The temporal coverage spans from August 1, 2021, to November 26, 2022, with all imagery captured via aircraft over the United States. RSTeller employed an automated workflow consisting of four main processes: (1) raw data acquisition from Google Earth Engine and OpenStreetMap (OSM), (2) raw caption generation using the Mixtral-7B large language model, (3) caption augmentation for linguistic diversity, and (4) quality control. The caption lengths varied from 5 to 192 tokens, with a median length of 48 tokens and an average of 54.2 tokens per caption. While RSTeller demonstrated the feasibility of large-scale automated dataset creation, its focus on NAIP imagery limited its diversity in terms of geographic coverage and image sources.

The RS5M [17] dataset, represented a major advancement in scale, providing a staggering 5 million image-text pairs. Its creation employed a two-stage methodology. First, a comprehensive filtering process was applied to 11 publicly available image-text datasets from the broader computer vision domain. This filtering stage, resulting in the PUB11 subset, involved text-based keyword filtering, de-duplication, and a dual-phase filtering process leveraging a pre-trained VLM to exclude images unrelated to RS. Second, the RS3 subset was constructed from existing class-labeled RS datasets, namely BigEarthNet-v1 [38], [39], FMoW [40], and MillionAID [41]. Descriptive captions were generated for these datasets using a pre-trained BLIP2 [42] model, and their quality was enhanced using a ranking system based on CLIP models and a novel rotational-invariance criterion. Finally, relevant meta-information, such as class labels, UTM coordinates, and UTC timestamps, were integrated into the captions, where available. The resulting RS5M dataset boasted a diverse range of image types, including both satellite and aerial perspectives, paired with descriptive English language captions often further enhanced with geographic, temporal, and scene-specific meta-information.

SkyScript [16], addressed the need for semantic richness by comprising 2.6 million image-text pairs with an impressive 29 thousand unique tags derived from OpenStreetMap (OSM). These tags detailed object categories, subcategories, and fine-grained attributes, providing a level of detail not found in previous datasets. SkyScript’s imagery was sourced from Google Earth Engine (GEE) collections, with spatial resolutions spanning 0.1m to 30m per pixel. The dataset’s global coverage favored regions with abundant high-resolution imagery and comprehensive OSM annotations, such as the U.S. and Europe. An automated annotation pipeline connected images to OSM data, employing a two-stage object selection for diverse representation, image selection based on object-specific criteria, and a two-stage tag classification using CLIP embeddings to ensure visual relevance and appropriate ground

sampling distance. Rule-based caption generation then synthesized OSM tags into descriptive captions, while a final filtering step, based on CLIP-derived image-text similarity, refined the dataset’s quality. While SkyScript represented a significant advancement in terms of semantic richness and automated annotation, its coverage bias towards regions with rich OSM data presented a limitation.

LuojiaHOG [43], focused on RS image-text retrieval, offering a dataset of 94,856 images sourced from Google Earth, covering diverse regions globally. A key feature of LuojiaHOG was its hierarchical classification system aligned with Open Geospatial Consortium (OGC) standards, featuring 7 first-level, 21 second-level, and 131 third-level categories, allowing for extensibility and compatibility with various data under different requirements. The dataset employed a hybrid annotation approach, combining manual and automatic processes. Manual annotation involved expert correction of OpenStreetMap (OSM) labels and the creation of detailed image descriptions following specific guidelines. Automatic annotation utilized Minigt4 [44] with prompt engineering to generate a large volume of image descriptions, with quality control measures implemented. Statistical analysis revealed an average caption length of 123.56 words and 6.95 sentences per caption. While LuojiaHOG’s hierarchical structure and detailed annotations are valuable, the hybrid annotation approach still involved significant manual effort and limited its scalability.

Hu et al. [45] introduced RSI-CAP and RSIEval, two interconnected datasets designed for training and evaluating vision-language models in RS. RSICap consists of 2,585 high-quality, human-annotated captions. The dataset included imagery derived from the DOTA [46] object detection dataset, featuring different satellite and aerial sensors such as GF-2, JL-1 and Google Earth, encompassing both color and panchromatic images with a wide range of spatial resolutions. The annotation process followed specific guidelines, including describing image attributes, object attributes, and overall scene, as well as including reasonable speculations based on visual content. RSICap captions have an average length of 60 words. RSIEval, on the other hand, was designed for benchmarking VLMs on RS image captioning (RSIC) and visual question answering (RSVQA) tasks. It contains 100 high-quality image-caption pairs (following RSICap annotation guidelines) and 936 diverse image-question-answer triplets, averaging nine questions per image. The questions covered four categories: object-related, image-related, scene-related, and reasoning-related. While RSI-CAP and RSIEval provided valuable resources for training and evaluation, their reliance on manual annotation limited their scalability.

ChatEarthNet [47], utilized ChatGPT-3.5 and ChatGPT-4V to generate 163,488 and 10,000 image-text pairs from Sentinel-2 imagery, respectively. The imagery featured global coverage and diverse temporal distribution across all continents except Antarctica, including nine spectral bands. Semantic information was derived from the ESA WorldCover project, which provides land cover maps at 10-meter resolution with 11 classes. ChatEarthNet features detailed natural language descriptions for each image, guided by prompts that incorporated land cover proportions and spatial distributions,

offering a mean of 90 words per caption for ChatGPT-4V and 155 for ChatGPT-3.5. While ChatEarthNet demonstrated the potential of large language models for automated caption generation, its reliance on specific data sources (Sentinel-2 and ESA WorldCover) still presented limitations in terms of diversity.

Muhtar et al. [48] introduced two new datasets: LHRS-Align and LHRS-Instruct. LHRS-Align is a large-scale dataset of 1.15 million RS image-caption pairs. Images, sourced from Google Earth at 1m resolution, were paired with geographic features from OpenStreetMap (OSM). The dataset’s annotation pipeline involved geo-aligning images with OSM features, pruning irrelevant attributes, and generating captions using Vicuna-v1.5-13B. LHRS-Instruct is a multi-modal instruction-following dataset for RS image understanding, including diverse tasks and complex visual reasoning data generated by GPT-4. The dataset was created by forming instruction datasets from public RS caption datasets (RSITMD [9] and NWPU [29]) through data cleaning and conversation generation with Vicuna-v1.5-13B, and selecting 15,000 LHRS-Align images, calculating bounding boxes from OSM data, and using GPT-4 to create complex instruction data. While LHRS datasets offer a high degree of automation and addressed diverse tasks, the reliance on specific language models and the manual construction of the benchmark dataset highlighted ongoing challenges.

Finally, Liu et al. [49] introduced Git-10M, a large-scale RS image-text dataset containing 10 million pairs, sourced by 30% from public datasets (Million-AID [41], GeoPile [50], SSL4EO-S12 [51], SkySript [16]) and 70% from Google Earth imagery. The dataset spans diverse geographical regions globally and includes various spatial resolutions ranging from 0.5m to 128m/pixel and geospatial metadata. They authors employ an automated annotation pipeline using GPT-4o, with prompts incorporating included geospatial metadata to generate semantically accurate descriptions.

In conclusion, the evolution of image-text paired datasets in RS has been marked by a progression towards larger scales, increased diversity, and greater automation. Early datasets like UCM-Captions and Sydney-Captions laid the groundwork for RS image captioning but suffered from limited diversity and relied heavily on manual annotation. Subsequent datasets like RSICD, RSITMD, and NWPU-Captions expanded the scale and introduced more fine-grained descriptions, but manual annotation remained a significant bottleneck. The emergence of datasets like RSVG, RSTeller, RS5M, SkyScript, LuoHOG and Git-10M represented a shift towards semi-automated and fully automated annotation approaches, leveraging techniques like language models, rule-based systems, and filtering based on visual-language models. However, challenges persist in terms of scalability, the labor and expertise required for annotation (even in semi-automated approaches), and the need for datasets that are both diverse and specific to the unique characteristics of RS imagery. Addressing these challenges will require continued research into novel annotation methodologies, the development of more sophisticated vision-language models tailored for RS, and the creation of comprehensive benchmarks that capture the full spectrum of

RS tasks.

### C. The imperative need for better annotations

The performance and efficacy of VLMs are critically dependent on two key factors: the sophistication of their architectural design and the quality, diversity, and scale of the training data. OpenAI’s CLIP [11], for instance, revolutionized the field with its unprecedented ability to bridge vision and language modalities, setting a new benchmark for multi-modal learning. However, while the model weights were made publicly available, the specific dataset used for training remains undisclosed, leaving a gap in the understanding of the data-driven foundations of its success. LAION-AI with OpenCLIP [52], the open-source implementation of OpenAI’s CLIP [11], has demonstrated impressive results. They managed to replicate OpenAI’s proprietary pre-training dataset [3] and subsequently trained and published several models [53], using various architectures, on a variety of data sources and compute budgets, ranging from small to large-scale experiments. Recent advancements in the context of CLIP pre-training have showcased remarkable achievements along the axes of pre-train data refinement [4], [54], [55], model architecture [56] and computational efficiency [57]–[59], leading to substantial improvements and eventually establishing new standards within the era of pre-trained CLIP models.

Despite the appeal of web-scraped image-text data as a cost-effective resource for encoding general knowledge, their inherent noise and the finite nature of the internet archive itself pose significant limitations. Recognizing that data quality often supersedes sheer quantity [60], recent works have been focusing on refining these datasets through advanced filtering and annotation improvement techniques. This pursuit has been significantly accelerated by the advent of foundation models, which have enabled a new wave of innovative approaches to filter and enhance existing datasets.

Early endeavors concentrated on the expansion of datasets through the incorporation of synthetic captions. A pioneering effort in this direction was the creation of LAION-COCO [61], a dataset encompassing 600 million synthetic captions derived from the LAION2B-en dataset. This work underscored the viability of employing synthetic data to augment the breadth and heterogeneity of image-text datasets.

Subsequent investigations have explored a variety of techniques aimed at refining and augmenting existing datasets. One prominent approach involves improving the caliber of captions through the utilization of sophisticated language models. For instance, Fan et al. [62] proposed a method to improve the quality of captions by leveraging language rewrites. They used a large language model, specifically GPT-3, to rewrite existing captions in the Conceptual Captions and SBU Captions datasets, focusing on improving the descriptiveness and accuracy of the text. This method was shown to improve the performance of CLIP models on downstream tasks, demonstrating the importance of high-quality captions for contrastive language-image pre-training.

Concurrently, Nguyen et al. [63] focused on refining existing captions in multimodal datasets to improve the training

TABLE I  
SUMMARY OF REMOTE SENSING IMAGE-TEXT PAIRED DATASETS

Dataset	Year	Images	Image-Text Pairs	Resolution (m/pixel)	Source(s)	Annotation Method
UCM-Captions [7]	2016	2,100	10,500	0.3	USGS National Map Urban Area Imagery	Manual
Sydney-Captions [7]	2016	613	3,065	0.5	Google Earth	Manual
RSICD [8]	2017	10,921	54,605	Variable	Google Earth, Baidu Map, MapABC, Tianditu	Manual
TextRS [31]	2020	2,144	10,720	Variable	AID, UC Merced, PatternNet, NWPU	Manual
RSITMD [9]	2022	4,743	23,715	Variable	RSICD, Google Earth	Manual
NWPU-Captions [29]	2022	31,500	157,500	30 – 0.2	NWPU-RESISC45	Manual
RSVGD [10]	2023	17,402	38,320	0.5 – 30	DIOR	Hybrid
Hephaestus [35]	2023	19,919	19,919	100	Comet-LiCS	Manual
RSI-CAP [45]	2023	2,585	2,585	Variable	DOTA, GF-2, JL-1, Google Earth	Manual
RSTeller [37]	2024	1.2M	2.5M	0.6	NAIP via Google Earth Engine	Automatic
RS5M [17]	2024	5M	5M	Variable	<b>PUB11 filtered datasets:</b> LAION-400M, YFCC100M CC3M, CC12M RedCaps, WIT TextCaps, VizWiz COCO, SBU Conceptual Captions  <b>RS3 datasets:</b> BigEarthNet-v1 FMoW MillionAID	Automatic
SkyScript [16]	2024	2.6M	2.6M	0.1 – 30	Google Earth Engine	Automatic
LuojiaHOG [43]	2024	94,856	94,856	Variable	Google Earth	Hybrid
ChatEarthNet [47]	2024	173,488	173,488	10	Sentinel-2, ESA WorldCover	Automatic
LHRS-Align [48]	2024	1.15M	1.15M	1	Google Earth, OSM	Automatic
Git-10M [49]	2025	10M	10M	0.5 – 128	30% public datasets (MillionAID, GeoPile, SSL4EO-S12, SkyScript), 70% Google Earth	Automatic
GAIA (ours)	2025	41,030	205,150	Variable	Several Remote Sensing-related websites	Automatic

of multimodal models. They utilized BLIP-2, a state-of-the-art vision-language model, to generate synthetic captions, and found that incorporating these captions during training led to significant performance gains in downstream tasks, further highlighting the importance of caption quality.

Another notable contribution in this area is the ShareGPT4V system [64], which aimed to enhance the performance of large multi-modal models through high-quality image captions. This approach involved fine-tuning a large language model on a carefully curated dataset of image-caption pairs, demonstrating the benefits of meticulously curated datasets for improving the performance of large-scale models. The study empirically showed that replacing just 3.5% of standard supervised fine-tuning data with their high-quality captions led to significant performance improvements in existing models like LLaVA-1.5 and Qwen-VL-Chat.

In a paradigm shift, Yu et al. [65] introduced CapsFusion, a novel approach that rethinks image-text data at scale. CapsFusion leverages an ensemble of captioning models, including BLIP, BLIP-2, and GIT, to generate a diverse set of captions

for each image. These captions are then fused using a large language model, specifically Vicuna-7B, to create a more comprehensive description. This method addresses the limitations of single-model captioning and demonstrates the advantages of leveraging multiple models to enhance caption quality.

Xu et al. [66] investigated the potential of alt-text as a valuable source of image descriptions. Their work, altogether, introduced a method for re-aligning alt-text with images, thereby leveraging this often underutilized information source. They employed a multi-stage training process involving human annotation and a specifically designed captioning model to enhance the alignment between alt-text and image content. This method was shown to improve image captioning performance, highlighting the value of alt-text in providing rich visual descriptions.

The application of synthetic data was further explored in specialized domains, such as medical vision-language pre-training. Liu et al. [67] investigated the feasibility of training effective medical vision-language models using purely synthetic data. They created a synthetic dataset of chest X-ray

images and reports using generative models and demonstrated that models trained on this synthetic data could achieve comparable performance to those trained on real data, thus addressing data scarcity and privacy concerns inherent in medical datasets.

Rotstein et al. [68] presented FuseCap, a system that leverages large language models to generate enriched, fused image captions. FuseCap employs frozen vision encoders, including an object detector, an attribute recognizer, and an OCR model, to extract detailed visual information from images. These outputs are then fused with original captions using a fine-tuned Flan-T5 model, resulting in comprehensive image descriptions. They curated a dataset of 12 million image-enriched caption pairs and demonstrated that training a BLIP-based captioning model on this data led to improved performance on downstream tasks.

Advancing the use of synthetic data, Sharifzadeh et al. [69] introduced a method that boosts visual-language models by utilizing synthetic captions and image embeddings. This approach employs a text-to-image model (MUSE) to generate synthetic image embeddings from captions generated by a large language model (LLaMA-3). They demonstrated that fine-tuning a VLM on this synthetic data achieves comparable performance to models trained on real data, highlighting the efficacy of combining different types of synthetic data.

Finally, Li et al. [70] undertook a large-scale experiment to investigate the capabilities of state-of-the-art language models in generating high-quality captions. They employed a LLaMA-3-powered LLaVA model to recaption 1.3 billion web images from the DataComp-1B dataset. Their results demonstrated significant improvements in the quality of the generated captions compared to the original web-crawled captions, highlighting the potential of advanced language models in large-scale data augmentation.

Despite these advancements, specialized fields such as medical imaging and remote sensing continue to face challenges due to the complex, domain-specific knowledge required for data curation, and the significantly lower tolerance for errors. In these high-stake domains, inaccuracies can have profound consequences. To this end, the medical domain has addressed this challenge by leveraging biomedical image-caption pairs, meticulously collected and filtered from various sources including open-access research publications [71]–[74], medical reports [75]–[77], and even social media platforms [78], [79], as a trustworthy source of paired image-text data. In contrast, the RS domain has been lately limited to publicly available annotation like land cover maps (e.g. ESA’s WorldCover) in conjunction with open-access RS imagery and large language models (LLMs) to generate grounded image-text pairs.

The research trajectory aimed at refining annotated datasets has dramatically progressed, yet challenges persist within specialized domains, particularly given their strict requirements for accuracy. Given the powerful capabilities of current foundation models, it is imperative for the RS community to explore and harness more effective priors. Drawing inspiration from the medical domain’s approach, the focus should shift towards leveraging these priors, and with the aid of the current ever-evolving foundation models, restructuring this information to develop more robust and adaptable in-domain

vision-language models.

### III. DESCRIPTION OF GAIA

#### A. Dataset Construction

To address the scarcity of high-quality, domain-specific image-text paired datasets in RS, we introduce GAIA, a novel dataset constructed through an automated, yet robust annotation pipeline depicted in Fig. 3 to advance RS image understanding and analysis. GAIA’s data collection pipeline involves targeted web-scraping of image-text pairs from reputable RS-related sources, followed by rigorous data cleaning and de-duplication, to ensure data integrity. For the data annotation part, we leverage ChatGPT and more specifically GPT-4o (omni). Through carefully crafted prompts, we instruct the model to extract domain-specific metadata and ultimately generate five distinct and diverse in-domain captions for each RS image, ensuring that each caption accurately interprets the visual data and provides semantically rich descriptions of the RS imagery. In contrast to existing RS image-text paired datasets that feature arbitrary RS imagery, GAIA provides a curated collection of semantically rich data. GAIA distinguishes itself through its global coverage, encompassing both anthropogenic and natural occurring events. This targeted approach enables the development of domain-specific VLMs capable of learning abstract representations that effectively encode the complex features and dynamic processes shaping our planet.

1) *Data Collection*: The data collection process was designed to be both comprehensive and efficient, ensuring high-quality and diverse data acquisition. We utilized custom web-scraping scripts to extract images and text from a curated list of reputable online sources which focus on the dissemination of Earth Observation articles that incorporate and analyze RS imagery. These sources were selected based on their data relevance, quality and diversity of content and are mainly comprised of online image repositories maintained by leading Earth Observation organizations. Due to the fact that most of these sources contain highly unstructured information, our web scraping efforts concentrated on extracting images, along with rich metadata and detailed descriptions, creating a solid foundation for subsequent annotation. We strictly adhered to the terms of service and licensing agreements of the respective sources. Our published dataset includes proper attribution to data providers and article authors within the metadata accompanying each sample. The sources utilized in this study, along with the respective counts of web-scraped articles, are summarized in Table II, while Table III provides an overview of the metadata fields collected for each sample, when available.

2) *Data Cleaning and De-duplication*: The raw web-scraped dataset underwent a data cleaning and de-duplication phase. Textual data was cleaned by removing HTML tags and URLs. To address instances of empty alt-text HTML tags, the corresponding article’s title was stored as a substitute of the original image caption. Image de-duplication was performed in two distinct phases. Initially, duplicate images were identified based on their source URLs. Subsequently, we utilized

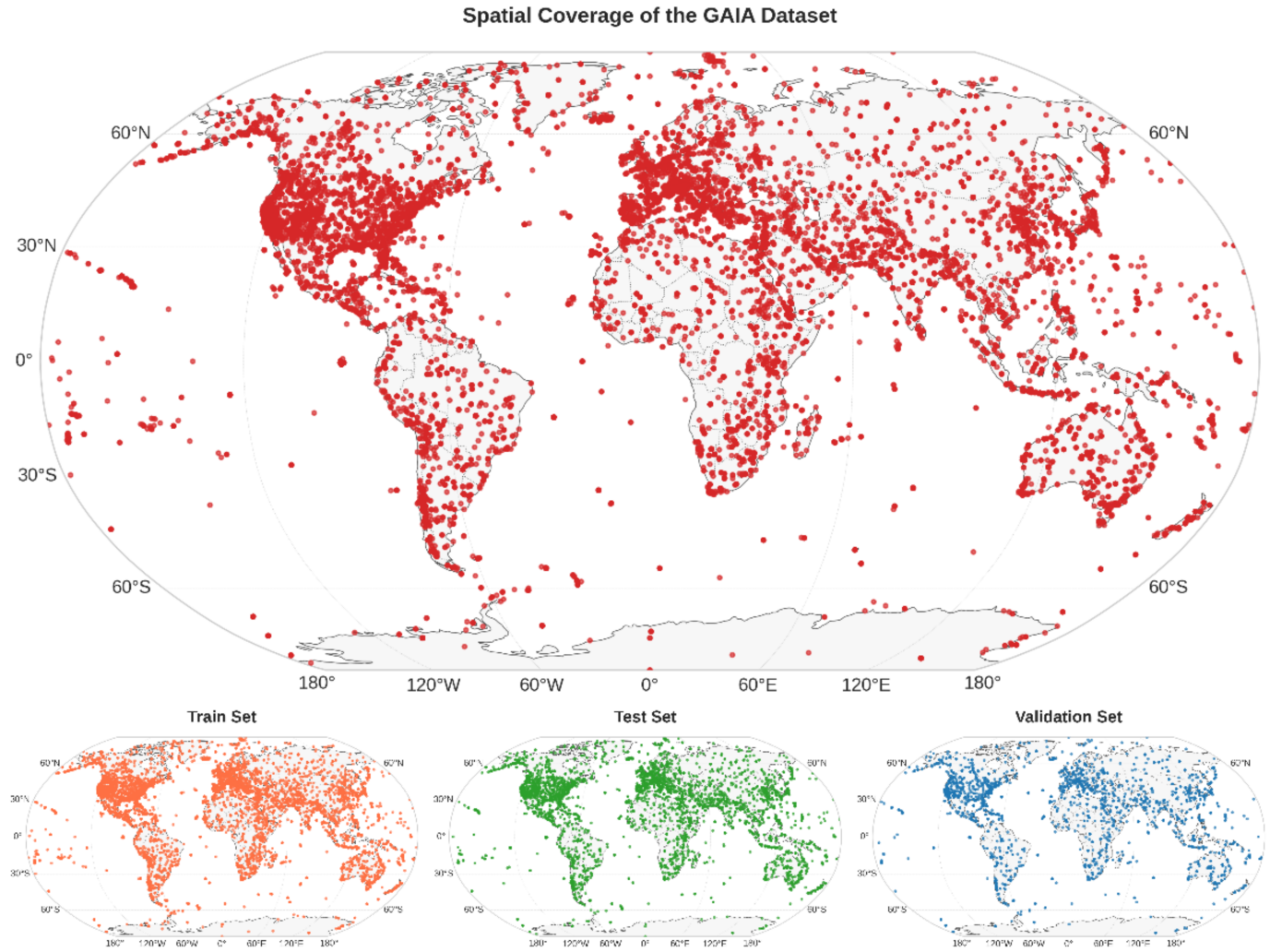


Fig. 2. Spatial coverage and distribution of the full GAIA dataset, in conjunction with the train, test, and validation sets. The main figure (top) illustrates the global spatial distribution of samples in the GAIA dataset. Each red dot represents a location associated with an image-text pair. The dataset exhibits broad coverage across various regions, with higher concentrations observed over North America, Europe, and parts of Asia and South America, including the often neglected Antarctic region. The three smaller maps (bottom) display the spatial distribution for the train set (orange), test set (green), and validation set (blue), respectively. This visualization demonstrates that the GAIA dataset provides a geographically diverse representation of Earth’s surface, which is crucial for training and evaluating robust RS models. The train, test, and validation sets maintain a similar spatial distribution pattern to the overall dataset, ensuring consistency across different data splits.

TABLE II  
ARTICLE COUNTS BEFORE AND AFTER FILTERING BY SOURCE

Source	Original	Filtered	% Retained
NASA	54,577	36,239	66.4
ESA	5,932	3,528	59.5
NOAA	651	455	69.9
AIRBUS	413	409	99.0
Planet	612	399	65.2
Total	62,185	41,030	66.0

fastdup<sup>3</sup>, an open-source tool for detecting visually similar images, to identify more duplicates, outliers, and corrupted images. In cases of duplication, dataset entries were merged, including their metadata, while outliers and corrupted images

were eliminated from the dataset.

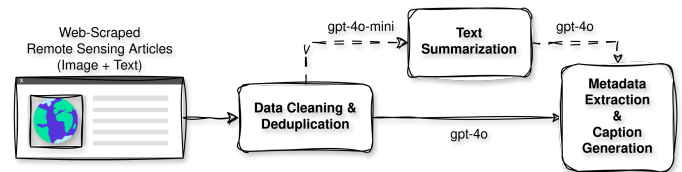


Fig. 3. Overview of GAIA data acquisition and annotation pipeline. This figure illustrates the process of building the GAIA dataset, from initial data acquisition to the generation of enriched metadata and captions. The pipeline begins with web-scraped RS articles (image + text) as the foundational data. This raw data undergoes a rigorous data cleaning and de-duplication process, which also involves text summarization using GPT-4o-mini in cases of large articles. Subsequently, GPT-4o is employed to extract metadata from the cleaned data and generate more descriptive captions, resulting in the comprehensive GAIA dataset.

<sup>3</sup><https://github.com/visual-layer/fastdup>

3) *Data Annotation Pipeline*: To facilitate the extraction of relevant metadata and the generation of comprehensive captions, a detailed prompt was developed to instruct ChatGPT and specifically their most capable model GPT-4o. The model was tasked with analyzing each RS image and its associated article’s text, extracting relevant domain-specific metadata, and generating five distinct, detailed captions per image. The prompt employed a system of rewards and penalties to reinforce desirable and discourage undesirable caption characteristics, respectively. Furthermore, a structured output schema was integrated to ensure consistent formatting and prevent omission of required fields or inclusion of hallucinated information. This structured approach promotes the extraction of domain-specific metadata and captions, enhancing consistency and facilitating downstream tasks such as dataset querying, filtering, and analysis. The systematic combination of detailed prompting and structured output contributed to the creation of a rich and informative dataset tailored for EO and RS applications. An overview of the extracted metadata fields and their descriptions is presented in Table III. For excessively long articles, a text summarization step was prepended to the data annotation pipeline. This involved utilizing the far more cost-effective, yet capable for the summarization task, GPT-4o-mini model to generate concise summaries, thereby mitigating annotation costs for the following annotation pipeline step while preserving the quality of extracted metadata and captions. Our qualitative analysis revealed that the geographic coordinates (EPSG:4326) generated by GPT-4o, while generally proximate, lacked the desired precision. Consequently, the GPT-4o generated coordinates were discarded in favor of those obtained from the Google Geocoding API <sup>4</sup>, which provides accurate latitude and longitude coordinates through toponym resolution.

4) *Overlap with Existing Datasets*: A key contribution of the GAIA dataset lies in its novelty, which was evaluated by quantifying its overlap with currently available web-crawled datasets (see Section II-A). Applying the consistent two-step data cleaning and de-duplication process outlined in Section III-A2, we determined that GAIA introduces a substantial proportion of previously unseen images. Specifically, less than 3% of GAIA’s images are found in the compared web-crawled datasets. These overlapping samples were deliberately retained, as GAIA provides five additional captions per image, augmenting the sources’ alt-text caption available in the existing datasets.

## B. Exploratory Data Analysis

This section presents a detailed exploratory data analysis of GAIA, delving into its temporal, spatial, and spectral characteristics, as well as the semantic content of its captions. The insights gained from this analysis, along with the illustration of GAIA dataset samples in Fig. 4, underscore the unique strengths and potential applications of the dataset for training and evaluating advanced VLMs.

Fig. 2 maps the spatial distribution of GAIA samples across the globe. GAIA exhibits a wide spatial coverage, with a concentration of samples over North America, Europe, and parts of Asia. This distribution reflects the availability of high-quality satellite imagery and the focus on regions with significant human activity and environmental change. The presence of samples in diverse geographic locations ensures that models trained on GAIA can learn to generalize across various landscapes, climates, and land cover types. In addition, GAIA’s stratified splits (train, test, and validation), shown in Fig. 2, fairly represent the global spatial coverage of the original dataset, with a balanced distribution across continents and regions. This fair representation across splits is crucial to avoid introducing biases during the training process and ensure that models can generalize well to unseen data from diverse geographical areas, while also ensuring a fair, thorough, and representative assessment of model performance during testing and validation.

GAIA’s temporal coverage spans over 25 years, from 1998 to 2024, providing a unique perspective on Earth’s changing landscapes. The distribution of samples across the years, shown in Fig. 5 (left), reveals a peak between 2001 and 2004. This surge can be attributed to the launch and operational years of key satellite missions, such as Terra/Aqua, that are widely present in the dataset. In addition, the increasing adoption of the Internet during the early 2000s likely also contributed to this trend. The rise of online data repositories, improved data sharing capabilities, and increased awareness towards RS applications. A subsequent decrease in sample count is observed after this peak, followed by a relatively uniform distribution from 2008 onwards, with a slight increase in the last decade. This more recent trend may also be related to the establishment of large initiatives for Earth Observation data collection and distribution, such as the European Union’s flagship Earth Observation Programme “Copernicus” in 2014. Fig. 5 (right) presents the monthly distribution of GAIA samples. The data exhibits a relatively uniform distribution across the months of the year, with a slight increase observed during the summer months in the Northern Hemisphere. This may be attributed to factors such as reduced cloud cover during summer, facilitating increased image acquisition opportunities, or a potential focus on capturing seasonally prominent phenomena like wildfires. The presence of data across all months ensures representation of diverse seasonal conditions within the dataset.

Fig. 6 shows the variety of satellite missions contributing to the GAIA dataset. In particular, GAIA includes images from more than 120 different satellite missions. The dominance of Terra/Aqua imagery (67.4%) is evident, reflecting its long operational history and wide range of applications. However, GAIA also incorporates data from a multitude of other missions, including Sentinel-2 (5.7%), Landsat (9.6%) and the Suomi NPP (3.0%), among others. Most interestingly, GAIA incorporates also images taken from the International Space Station (ISS) (3.0%). This sensor diversity enriches the dataset with various spatial resolutions, and viewing geometries, leveraging multiple spaceborne platforms and thus enabling the development of models that are adaptable to different data sources and capable of capturing a comprehensive view of

<sup>4</sup><https://developers.google.com/maps/documentation/geocoding/requests-geocoding>

TABLE III

METADATA FIELDS IN THE GAIA DATASET: WEB-SCRAPED AND SYNTHETICALLY-GENERATED. THE GAIA DATASET INCLUDES TWO TYPES OF METADATA: (1) ORIGINAL METADATA SCRAPED FROM WEB SOURCES DURING DATA COLLECTION, AND (2) ADDITIONAL METADATA GENERATED BY GPT-4O TO ENHANCE THE DATASET. THE TABLE IS DIVIDED INTO TWO SECTIONS TO REPRESENT EACH TYPE. THIS COMPREHENSIVE METADATA APPROACH PROVIDES RICH CONTEXTUAL INFORMATION FOR EACH DATA SAMPLE AND FACILITATES DETAILED ANALYSIS.

Part 1: Web-scraped Metadata	
Metadata Field	Description
id	Unique identifier for each data sample.
image_src	URL of the hosted image file.
image_alt	Original alt-text provided for the image.
datetime	Date and time associated with the image.
location	Geographic location associated with the image.
coordinates	Geographic coordinates (latitude, longitude) in EPSG:4326 format.
topics	Relevant keywords or subject tags.
satellite	Satellite used to acquire the image.
credits	Information on image data source, and text authorship.
Part 2: Synthetically-generated Metadata	
Metadata Field	Description
tag	Up to three domain-specific tags that describe the image.
location	Precise point location, preferably in 'Landmark, City, Country' format.
coordinates	Approximate geographical coordinates of the point location in EPSG:4326 format.
modality	Remote Sensing modalities or sensor types used (e.g., Optical, Thermal).
satellite	Name of the Remote Sensing satellite (e.g., Sentinel-2).
sensor	Remote Sensing sensor/instrument used (e.g., MultiSpectral Instrument (MSI)).
resolution	Spatial resolution of the sensor: Low, Moderate, High, or Very High.

Earth's features.

GAIA's multi-modal nature is highlighted in Fig. 7, which displays the distribution of RS modalities. While optical/multispectral imagery constitutes the majority (88.1%), the dataset also incorporates thermal infrared (6.6%), radar (2.6%), microwave radiometry (1.0%), and near-infrared (0.5%) data, among others.

GAIA's imagery is characterized by a diverse range of spatial resolutions, categorized as low, moderate, high, and very high. As depicted in Fig. 8, the majority of the samples (85.8%) fall under the moderate resolution category. Moreover, the presence of high (12.2%) and very high (1.4%) resolution images allows for the exploration of fine-grained details. The negligible amount of low-resolution images (0.6%) suggests a focus on capturing Earth's surface with sufficient detail for meaningful analysis. This plethora of diverse spatial resolution imagery makes GAIA particularly well-suited for tasks requiring either balance between broad spatial coverage or detailed feature analysis, at various scales.

Fig. 9 presents a word cloud generated from the captions in the GAIA dataset, providing a glimpse into the rich semantic content captured within. Prominent terms such as "dust", "storm", "fires" and "satellite" highlight the dataset's focus on natural phenomena and RS-related concepts. The presence of geographic terms like "volcano", "island", and "ocean" underscores the diverse range of environments represented. This rich vocabulary enables the development of VLMs models that can generate detailed and contextually relevant descriptions, capturing both the physical characteristics and the underlying

processes shaping our planet.

Fig. 10 categorizes the semantic content of GAIA into the five Earth system domains: Atmosphere, Biosphere, Cryosphere, Geosphere, and Hydrosphere. Each domain is further divided into subcategories representing specific phenomena, processes, or features based on GAIA samples thematic tags. This hierarchical organization reflects the comprehensive nature of GAIA, covering a wide spectrum of Earth science topics and providing a valuable resource for training VLMs to describe a wide array of Earth science concepts.

Finally, Fig. 11 presents the distribution of image heights and widths within the GAIA dataset. Both height and width distributions exhibit a bell-shaped curve, with mean values of 2720 and 2867 pixels, and median values of 2542 and 2778 pixels, respectively. These values, in conjunction with the narrow distribution around the mean indicate that GAIA images are generally large, capturing extensive spatial information. The presence of images with larger dimensions, up to 10,000 pixels, indicates variability in scene coverage and potential level of detail.

Focusing on the textual characteristics of the GAIA dataset, a comparative analysis between the original alt-text captions and our synthetic captions, shown in Table IV, reveals significant differences in their richness and complexity. The synthetic captions exhibit a considerably larger vocabulary (28,751 vs. 16,173) and a higher number of unique words (Hapax Legomena of 7,862 vs. 6,543), indicating a more diverse and nuanced use of language. This enhanced lexical diversity is further emphasized by the substantially higher total

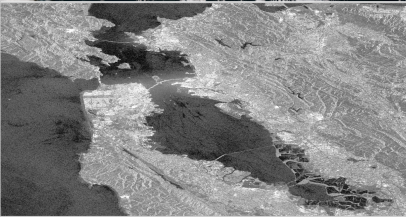
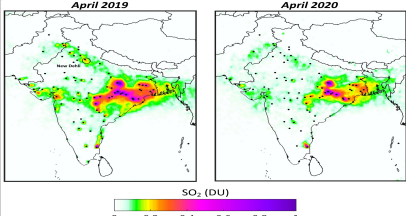
GAIA Dataset Samples		
Satellite Image	Original Alt-Text & Metadata	ChatGPT Captions
	<p><b>Location:</b> Bari, Italy  <b>Coordinates:</b> 41.1171432, 16.8718715  <b>Datetime:</b> 2022-07-22  <b>Satellite:</b> Pleiades  <b>Modality:</b> Optical  <b>Resolution:</b> Very High  <b>Tags:</b> Urban Planning, Infrastructure, Coastal City  <b>Credits:</b> Pleiades Neo Airbus DS 2022</p> <p><b>Alt-text:</b> Bari, Italy, Very High-Resolution Imagery</p>	<ol style="list-style-type: none"> <li>1. An intricate urban layout of Bari, Italy, captured using Very High-Resolution imagery from the Pleiades Neo satellite. The central area is densely packed with rectangular grid patterns typical of urban planning, indicating a well-developed infrastructure.</li> <li>2. A coastal cityscape of Bari, highlighting the juxtaposition of urban development against the Adriatic Sea. The harbor area is visible with distinct dock structures and water bodies, indicating significant maritime activity.</li> <li>3. Detailed land use patterns in Bari, illustrating residential, commercial, and industrial zones. The urban sprawl extends inward from the coast, with major roads intersecting the city, facilitating connectivity and transport.</li> <li>4. The spatial organization of Bari's urban environment, featuring notable landmarks such as sports facilities and green spaces. This layout supports recreational activities and enhances the quality of life for residents.</li> <li>5. Bari's urban morphology captured in the summer of 2022, with clear evidence of planned city growth. The coastal boundary is defined by protective harbor structures, indicating efforts in land administration and coastal management.</li> </ol>
	<p><b>Location:</b> Powell County, Kentucky  <b>Coordinates:</b> 37.8380647, -83.8260884  <b>Datetime:</b> 2021-03-11  <b>Satellite:</b> SkySat  <b>Modality:</b> Optical  <b>Resolution:</b> Very High  <b>Tags:</b> Flood, Floodplain Evaluation  <b>Credits:</b> Planet Labs</p> <p><b>Alt-text:</b> After the Flood</p>	<ol style="list-style-type: none"> <li>1. A floodplain along the Red River near Clay City, exhibiting residual floodwater in a true-color SkySat capture, highlighting land use patterns and water's interaction with the landscape.</li> <li>2. Curved river courses with lingering floodwater visible in the floodplain, aiding in post-flood impact assessment in Powell County, captured by high-resolution satellite imagery.</li> <li>3. A detailed examination of the flood aftermath with visible water traces on the floodplain, providing crucial insights for local officials and insurance evaluation.</li> <li>4. High-resolution visualization of residual water patches along the floodplain, captured by SkySat, offering key data for evaluating flood impact and recovery efforts.</li> <li>5. A landscape marked by receding floodwaters, with the spatial distribution of water evident in the floodplain, facilitating analysis of flood impact using Planet data.</li> </ol>
	<p><b>Location:</b> Gulf of Alaska, Alaska  <b>Coordinates:</b> 63.588753, -154.4930619  <b>Datetime:</b> 2017-11-16  <b>Satellite:</b> Suomi NPP  <b>Modality:</b> Optical  <b>Resolution:</b> Moderate  <b>Tags:</b> Glacial Dust, Phytoplankton Growth, Marine Ecosystems  <b>Credits:</b> National Oceanic and Atmospheric Administration NOAA</p> <p><b>Alt-text:</b> Glacial dust streams into the Gulf of Alaska</p>	<ol style="list-style-type: none"> <li>1. A plume of glacial dust extending into the Gulf of Alaska, originating from the Copper River Valley. The phenomenon is captured by the VIIRS instrument aboard the Suomi NPP satellite. The glacial flour, rich in iron, is visible as a distinct brownish streak over the ocean, highlighting the interaction between terrestrial and marine environments.</li> <li>2. The Gulf of Alaska with a prominent dust plume from the Copper River Valley, observed by the Suomi NPP satellite's VIIRS instrument. The glacial dust, known as rock flour, is dispersed by strong winds over the ocean, potentially influencing phytoplankton blooms due to its iron content.</li> <li>3. Atmospheric dispersion of glacial dust into the Gulf of Alaska, a process visible through the VIIRS sensor on the Suomi NPP satellite. The dust, originating from dried riverbanks, contributes to marine nutrient cycles, impacting regional marine ecosystems.</li> <li>4. The interplay between land and sea as glacial dust from the Copper River Valley is carried into the Gulf of Alaska, captured by the Suomi NPP satellite using its VIIRS sensor. This event demonstrates the significant role of aeolian processes in nutrient distribution across marine environments.</li> <li>5. A sweeping view of glacial dust from the Copper River Valley over the Gulf of Alaska, observed by the VIIRS instrument on the Suomi NPP satellite. This natural dust transport mechanism is key to understanding nutrient dynamics and ecosystem changes in the region."</li> </ol>
	<p><b>Location:</b> San Francisco Bay, California  <b>Coordinates:</b> 37.8271784, -122.2913078  <b>Datetime:</b> 2009-12-09  <b>Satellite:</b> RADARSAT  <b>Modality:</b> Radar  <b>Resolution:</b> Moderate  <b>Tags:</b> Oil spill, Marine pollution  <b>Credits:</b> RADARSAT-1 data ©2007 Canadian Space Agency</p> <p><b>Alt-text:</b> November 12, 2007</p>	<ol style="list-style-type: none"> <li>1. Oil slicks prominently visible in San Francisco Bay, captured using radar imagery. The oil is seen as dark areas, contrasting with brighter land and rougher water surfaces due to reduced surface tension caused by the spill.</li> <li>2. Spread of oil north and west in San Francisco Bay, encircling Angel Island. Smooth, dark patches on the water indicate oil presence, visible in radar imagery due to its ability to detect textural differences.</li> <li>3. A significant oil spill extending from San Francisco Bay into the Pacific Ocean. Long ribbons of oil south of the Bay Bridge are visible, illustrating the impact of tidal movements on oil dispersion.</li> <li>4. Environmental impact on marine habitats, with oil spreading over 30 kilometers of shoreline. Radar imagery reveals smoother water surfaces where oil is present, affecting nearby wildlife and ecosystems.</li> <li>5. Radar detection of oil slicks near urban areas and natural reserves. The contrast between oil-darkened water and brighter urban land highlights the spill's extent and the ongoing clean-up efforts visible through ships in the bay.</li> </ol>
	<p><b>Location:</b> India  <b>Coordinates:</b> 20.593684, 78.96288  <b>Datetime:</b> 2022-07-22  <b>Satellite:</b> Sentinel-5P  <b>Modality:</b> Optical  <b>Resolution:</b> Low  <b>Tags:</b> Sulfur Dioxide, Air Pollution, Power Plants  <b>Credits:</b> Copernicus data (2019-20), processed by BIRA-IASB.</p> <p><b>Alt-text:</b> SO2 concentrations and location of power plants in India</p>	<ol style="list-style-type: none"> <li>1. Comparative maps of sulfur dioxide concentrations over India for April 2019 and April 2020, captured by the Sentinel-5P satellite. Darker shades indicate higher SO2 levels, concentrated mainly around coal-fired power plants denoted by black dots.</li> <li>2. A visual analysis of SO2 pollution across India, with significant reductions from April 2019 to April 2020, possibly due to decreased industrial activity during the COVID-19 lockdown. High concentrations are visible in eastern and central regions.</li> <li>3. Temporal changes in atmospheric sulfur dioxide levels over India, with a noticeable decline from 2019 to 2020. The spatial distribution highlights major industrial zones, and the black dots mark the locations of large power plants.</li> <li>4. Sulfur dioxide distribution in India, with the Sentinel-5P data illustrating a shift in pollution patterns. April 2020 shows lower concentrations, suggesting an impact from reduced industrial emissions amid COVID-19 restrictions.</li> <li>5. Remote sensing data from Sentinel-5P revealing the spatial and temporal dynamics of SO2 emissions in India. The maps highlight a clear reduction in SO2 levels in 2020, during the COVID-19 lockdown, particularly in areas with clustered power plants.</li> </ol>

Fig. 4. A glimpse into the GAIA dataset, showing various satellite images alongside metadata, the original alt-text and our five descriptive synthetic captions. This diverse content highlights the dataset's heterogeneity, as well as the enhanced descriptive richness achieved through our synthetic captions.

word count in the synthetic captions (7,493,402 vs. 394,471). Furthermore, the average number of words per caption is significantly greater for the synthetic (36.53) compared to the original alt-text (9.61), with a lower standard deviation (7.23 vs. 12.48), suggesting not only longer but also more consistently detailed descriptions. Each image is associated with five synthetic captions, compared to a single alt-text caption, resulting in a fivefold increase in the total number of captions and offering a diverse textual representation of each scene.

#### IV. EXPERIMENTS

##### A. Experimental Setup

For our classification and cross-modal retrieval experiments, we utilized CLIP [11] pre-trained vision transformer (ViT) models [80]. The models were loaded using the OpenCLIP library [52]. Our evaluation methodology followed the setup

described in [11] and utilized the CLIP Benchmark<sup>5</sup> evaluation suite to ensure a consistent and fair comparison with existing zero-shot CLIP benchmarks. Classification performance was assessed using Accuracy (Acc1 and Acc5) and Mean Recall, while the retrieval task performance was evaluated using Recall@K (R@K).

For our image captioning experiments, we employed the BLIP2 [42] pre-trained model, specifically opting for its smallest and most resource-efficient variant, the blip2-opt-2.7b model. This choice allowed us to focus on fine-tuning the model exclusively using our image-caption paired dataset, eliminating the need for additional instruction tuning datasets, as required by models like LLaVA [81], [82]. To evaluate image captioning performance, we employed commonly used metrics, including BLEU [83], ROUGE-1, ROUGE-2,

<sup>5</sup>[https://github.com/LAION-AI/CLIP\\_benchmark](https://github.com/LAION-AI/CLIP_benchmark)

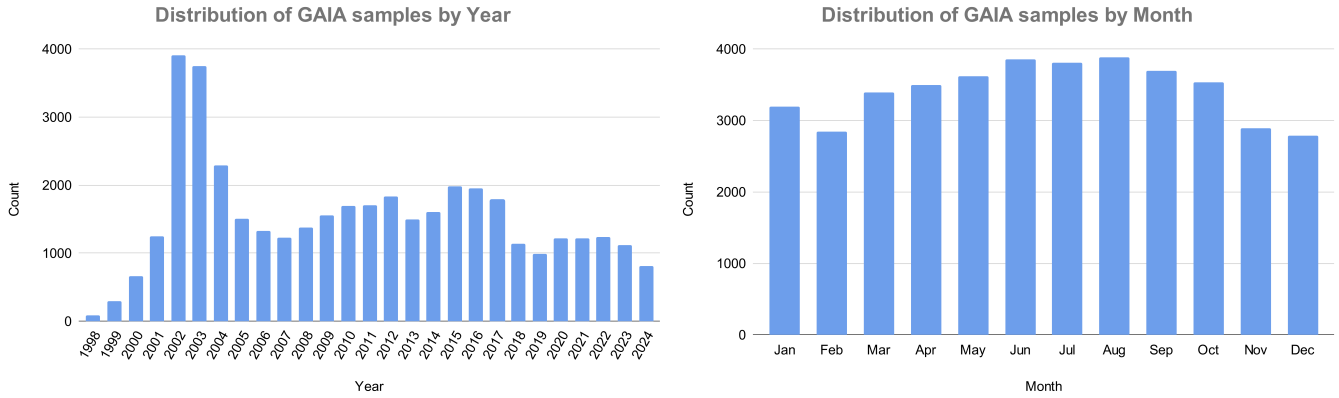


Fig. 5. Temporal distribution of samples within the GAIA dataset. (a) Yearly distribution of image-text pairs in GAIA, covering a period of over 25 years from 1998 to 2024. A pronounced peak in data volume is evident between 2001 and 2004. This peak coincides with the operational periods of significant satellite missions like Terra/Aqua and the increasing availability of RS data through online repositories, due to the internet uptake. A relatively uniform distribution is observed from 2008 onwards, with a slight upward trend in the last decade potentially associated with initiatives like the Copernicus Programme. (b) Monthly distribution of GAIA samples, demonstrating a relatively even representation across all months. A minor increase in sample count during the Northern Hemisphere’s summer months is observed, potentially linked to reduced cloud cover and a focus on capturing seasonal phenomena such as wildfires. The consistent presence of data throughout the year ensures that GAIA captures a comprehensive range of seasonal variations.

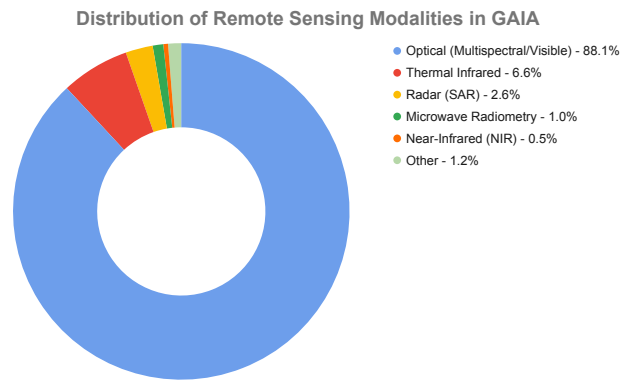
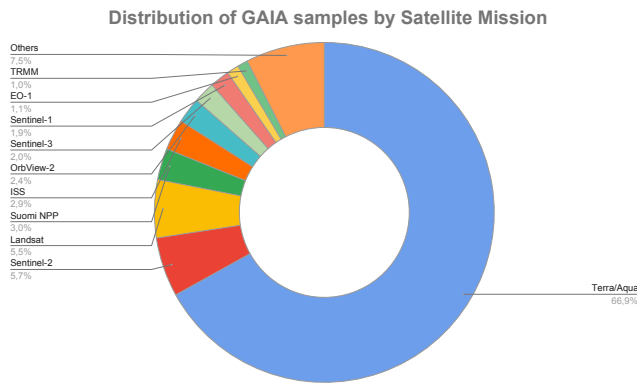


Fig. 6. The chart illustrates the contribution of various satellite missions to the GAIA dataset. Notably, Terra/Aqua missions are the most represented, accounting for 66.9% of the data, attributable to their extensive operational history and broad application range. Other significant contributions come from missions such as Sentinel-2 (5.7%), Landsat (5.5%), and Suomi NPP (3.0%) and the International Space Station (ISS) (2.9%). “Others” represents the combined contribution of the remaining satellite missions (7.5%). All in all, the dataset includes images from over 120 satellite missions. This diversity in sensor data, including variations in spatial resolution, spectral bands, and viewing geometries, ensures a rich dataset for training and evaluating RS VLMs.

Fig. 7. The chart illustrates the proportion of different RS modalities represented in the GAIA dataset. Optical (multispectral/visible) imagery is the most prevalent, comprising 88.1% of the dataset. Thermal infrared data accounts for 6.6%, while radar (SAR) data contributes 2.6%. Microwave radiometry and near-infrared (NIR) modalities are also present, representing 1.0% and 0.5% of the dataset, respectively. The “Other” category, encompassing less frequent modalities, accounts for 1.2%. This multi-modal nature of GAIA enables the capture of a wider range of Earth phenomena beyond the visible spectrum, potentially leading to more informative and accurate image-text descriptions for various RS applications.

ROUGE-L [84], and METEOR [85], ensuring a comprehensive assessment of the model’s capabilities.

We created three dataset splits (train, test, and validation - see Fig. 2) with a 70/20/10 ratio, spatio-temporally stratified. Temporal stratification was based on grouping GAIA samples into seasons according to their acquisition date. Spatial stratification was achieved using Geohash [86], a hierarchical geocoding system that partitions the Earth’s surface into a grid of cells. A Geohash precision of 3 was used, corresponding to a grid cell size of approximately  $156km \times 156km$ . The stratified global spatial and temporal coverage of these splits is illustrated in Fig. 2.

Fine-tuning of both the CLIP models and the BLIP2 was performed on a single Nvidia GeForce RTX 4090 GPU. For the CLIP models fine-tuning, the predefined train split of our dataset was used with a batch size of 128 for a single epoch. For the single alt-text captions we perform fine-tuning as usual, while for the five synthetic captions, we incorporate an intermediate step where we average the embeddings of all five captions to produce a unified representation. We employed a learning rate of  $5e-6$  with a 10% warmup ratio, a cosine annealing learning rate schedule, and the AdamW optimizer [87], [88] with a weight decay of 0.1 [89]. Gradient checkpointing [90] was enabled for the largest models to accommodate memory constraints without reducing the batch

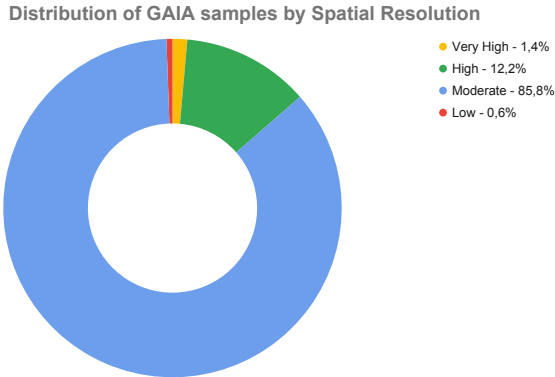


Fig. 8. The chart depicts the distribution of spatial resolutions within the GAIA dataset, categorized as Very High (less than 1m), High (1-10m), Moderate (10-100m), and Low (greater than 100m). Moderate-resolution imagery is the most prevalent, constituting 85.8% of the dataset. High-resolution and Very High-resolution data account for 12.2% and 1.4% respectively, while Low-resolution imagery represents a smaller fraction at 0.6%. This distribution highlights GAIA’s emphasis on moderate-resolution data, which offers a balance between spatial detail and coverage area, making it suitable for a wide array of RS tasks. The inclusion of higher and lower resolution data further adds to the dataset’s versatility, allowing for analyses at various scales, from broad spatial coverage to detailed feature analysis.

TABLE IV  
COMPARATIVE STATISTICS OF TEXTUAL DESCRIPTIONS IN THE GAIA DATASET: ALT-TEXT VS. SYNTHETIC.

Attribute	Alt-Text	Synthetic
<b>Vocabulary</b>		
Size	16,173	28,751
Hapax Legomena	6,543	7,862
Total Words	394,471	7,493,402
<b>Words per Caption</b>		
Minimum	1	12
Maximum	182	84
Average	9.61	36.53
Median	6.0	36.0
Standard Deviation	12.48	7.23
<b>Sentences</b>		
Avg. per Caption	1.05	1.87
Total	43,208	383,885
<b>Captions</b>		
Total	41,030	205,150

size. No data augmentation techniques were employed. During fine-tuning, both the vision and text encoders remain trainable, and no additional trainable parameters were introduced to the models. For BLIP-2 model fine-tuning, we adopted a parameter-efficient approach using Low-Rank Adaptation (LoRA) [91]. The model was fine-tuned on the predefined training split of our dataset using a batch size of 16 over five epochs. LoRA was applied to the attention layers with a rank of 16, a scaling factor  $\alpha$  of 32, and a dropout rate of 0.1. Unlike our CLIP fine-tuning methodology, which averages the text embeddings from the five synthetic captions to generate

a unified text representation, we adopted a sampling approach for BLIP-2. During fine-tuning, a single caption was randomly selected per image at each epoch. This strategy preserves caption diversity while mitigating overfitting risks. Similarly to the CLIP setup, no data augmentation was applied.

Ultimately, we assessed classification performance on three benchmark datasets featured in the CLIP [11] benchmark suite, enabling direct comparisons across datasets: (1) two RS scene classification datasets, EuroSAT and RESISC45, and (2) ImageNet1K, a well-established general-domain benchmark where CLIP models typically achieve strong performance. RS scene classification, is one of the few tasks presented by the CLIP authors, where zero-shot CLIP significantly underperforms on the EuroSAT and Resisc45 datasets, resulting in some of the biggest deltas (-37.1% and -11.9% respectively) among all tasks assessed, when compared to a fully supervised ResNet50 baseline model. By including ImageNet-1K, we aimed to investigate the impact of GAIA fine-tuning on CLIP’s retained capabilities in tasks where its baseline performance is already robust. For the evaluation of cross-modal retrieval and image captioning, we employed the GAIA test split. We performed a comparative analysis of cross-modal alignment performance, assessing the performance both before and after fine-tuning, and contrasting the outcomes for alt-text captions against those obtained using synthetic captions. This allowed us to quantify the performance gains associated with each captioning approach. Furthermore, for image captioning assessment, we evaluated two key aspects. We first quantified the performance improvement resulting from fine-tuning compared to zero-shot performance. Secondly, we analyzed the performance enhancements associated with each individual captioning scheme.

## B. Experimental Results

We present the results of our CLIP experiments in Table V and Table VI, for classification and retrieval, respectively. Both tables highlight the benefits of fine-tuning CLIP models with GAIA, i.e. using semantically rich image-text paired datasets, for both classification and cross-modal retrieval. More specifically, Table V reveals that fine-tuning, caption quality, and model scale emerge as key factors significantly influencing CLIP classification performance. ImageNet1k demonstrates the highest performance, while RS datasets benefit the most from fine-tuning, indicating the need for domain adaptation. Synthetic captions have a positive impact on classification, providing substantial improvements compared to alt-text captions. Significant Acc1, Acc5, and Mean Recall gains are observed post fine-tuning, especially for EuroSAT, addressing the known zero-shot CLIP under-performance in RS. For Resisc45 on the other hand, while fine-tuning influences the vast majority of the 45 dataset classes positively, in terms of evaluation metrics, it affects negatively classes such as "Airplane", "Airport", "Church", leading to marginal performance gains overall. These modest performance gains could be attributed to the GAIA dataset thematics as well as the limited representation of "very high" and "high" spatial resolution imagery in the dataset, as shown in Fig. 8. Importantly, fine-tuning on GAIA does not degrade ImageNet1k performance



tive examples to understand the capabilities and limitations of the fine-tuned models. The evaluation metrics, summarized in Table VII, reveal a clear improvement in captioning performance after fine-tuning BLIP2 on the GAIA dataset. Both fine-tuning approaches, using either alt-text or synthetic captions, significantly outperform the zero-shot BLIP2 model across all metrics (BLEU, ROUGE-1, ROUGE-2, ROUGE-L, METEOR). Fine-tuning substantially improves performance. Models fine-tuned on GAIA’s synthetic captions consistently outperform those fine-tuned on alt-text captions. This suggests that the richer and more semantically meaningful synthetic captions provide a better training signal in order for BLIP2 to learn to produce more nuanced in-domain descriptions. The most significant improvements are observed in ROUGE and METEOR scores, which are more sensitive to semantic similarity and recall, while BLEU, focused on precision and n-gram overlap, shows a lower absolute improvement but still a notable relative gain. This indicates that fine-tuning helps BLIP2 generate captions that are more semantically similar to the reference captions, although n-gram overlap (BLEU) might still be relatively limited. Overall, the quantitative metrics strongly indicate that fine-tuning BLIP2 on GAIA dataset, especially using synthetic captions, significantly enhances its RS image captioning capabilities.

A qualitative analysis of the generated captions (see Fig. 12) provides deeper insights into the fine-tuned model’s strengths and weaknesses, which might be traced back to GAIA and reveal potential limitations or potent areas for improvement. Fine-tuned models, particularly those trained on synthetic captions, generate predictions that are more relevant to the image content and reference captions compared to zero-shot predictions. They are better at identifying key elements, locations, and events described in the references captions. Moreover, GTP-4o fine-tuned models show improved ability to handle complex RS scenes, such as those involving natural disasters (wildfires, floods, cyclones) and environmental phenomena (phytoplankton blooms, dust storms). They more accurately identify these events compared to their other two counterparts. Last but not least, models fine-tuned using our synthetic captions generate prominently more extensive and informative descriptions.

Despite those improvements, fine-tuned models occasionally hallucinate or generate inaccurate details. The models sometimes misidentify locations, confusing geographically proximate but distinct places. This suggests a challenge in precisely grounding the captions geographically, even after fine-tuning. Moreover, while the models generally improve in correctly identifying the broad modality of RS imagery (e.g., optical, radar), they still confuse specific sensors and missions. For instance, a caption might misidentify “Sentinel-2” for “MODIS” or most trivially correctly identify “MODIS” but incorrectly attribute it to “Terra” instead of “Aqua,” or vice versa. Lastly, models fine-tuned on synthetic captions, while generating more informative descriptions, sometimes produce captions that are excessively verbose or redundant, indicating a need for better control over caption length and conciseness.

## V. DISCUSSION AND CONCLUSION

In this paper, we introduced GAIA, a novel global, multi-modal, multi-scale vision-language dataset for RS image analysis. GAIA addresses the crucial need for high-quality, domain-specific data to advance the development and application of VLMs in RS. Through a carefully designed data acquisition and annotation pipeline, leveraging web-scraping and the advanced language generation capabilities of GPT-4o, we have created a dataset of remarkable scale, diversity, and semantic richness within the RS domain. Our exploratory data analysis and experimental results robustly demonstrate GAIA’s unique characteristics and effectiveness in improving the performance of VLMs on RS tasks. The dataset’s global coverage, multi-modal nature, and focus on diverse Earth events, coupled with its scientifically grounded synthetic captions, make GAIA a valuable resource for the RS community.

The release of the GAIA dataset, alongside the automated processing framework and pre-trained model weights, aims to democratize access to high-quality RS vision-language data and accelerate research in this rapidly evolving field. We believe that GAIA will pave the way for the development of more robust, generalizable, and impactful VLMs for RS, enabling new approaches to Earth observation data analysis and unlocking deeper insights into our planet’s dynamic systems. Future work will focus on expanding the dataset’s scale and thematic scope, further refining annotation quality, exploring its utility across a wider range of VLM architectures and downstream applications, and ultimately, leveraging GAIA to advance the development of next-generation foundation models for RS.

### A. Bridging the gap between Remote Sensing and Vision-Language Models

Our investigation into the current landscape of VLMs and RS datasets revealed a critical gap: existing VLMs, predominantly trained on generic web data, exhibit limited proficiency in the specialized domain of RS, and publicly available RS datasets often lack the scale, diversity, and annotation quality necessary to bridge this gap. GAIA directly addresses these shortcomings through a meticulous two-stage construction process, combining targeted web-scraping from reputable RS sources with advanced caption generation using GPT-4o. This approach has yielded a dataset of 205,150 high-quality image-text pairs, characterized by its global, multi-modal, and multi-scale nature, and importantly, its focus on capturing diverse Earth events and phenomena.

GAIA exhibits a balanced spatial and temporal distribution, spanning 25 years of Earth observations across diverse geographic regions. The inclusion of imagery from over 120 satellite missions and a variety of RS modalities, predominantly optical but also incorporating thermal, radar, and other spectral data, ensures a rich and heterogeneous visual resource. The predominance of moderate-resolution imagery, supplemented by high and very-high resolution data, provides versatility for a wide range of RS analysis tasks, from broad area monitoring to detailed feature extraction. Furthermore, the semantic analysis of GAIA’s captions, visualized through word clouds

TABLE V  
CLASSIFICATION RESULTS GROUPED BY MODEL AND CAPTION SCHEME PRE AND POST FINE-TUNING WITH EITHER OF THE GAIA CAPTION SCHEMES

	Dataset	Model	Captions	Mode	Metrics (%)		
					Acc1	Acc5	Mean Recall
eurosat	ViT-B-32	Alt-text	Zero-shot	50.46	92.41	49.06	
			Fine-tuned	61.20	95.72	60.87	
		Synthetic	Zero-shot	50.46	92.41	49.06	
			Fine-tuned	62.04	95.72	61.35	
	ViT-L-14	Alt-text	Zero-shot	62.57	95.93	63.95	
			Fine-tuned	68.76	98.39	70.09	
		Synthetic	Zero-shot	62.57	95.93	63.95	
			Fine-tuned	72.52	98.93	72.84	
	ViT-L-14-336	Alt-text	Zero-shot	61.52	96.06	62.97	
			Fine-tuned	67.02	99.04	68.57	
		Synthetic	Zero-shot	61.52	96.06	62.97	
			Fine-tuned	74.22	99.20	74.16	
resisc45	ViT-B-32	Alt-text	Zero-shot	53.65	86.71	54.08	
			Fine-tuned	50.97	84.02	51.29	
		Synthetic	Zero-shot	53.65	86.71	54.08	
			Fine-tuned	55.57	86.81	56.27	
	ViT-L-14	Alt-text	Zero-shot	63.35	92.40	63.82	
			Fine-tuned	63.89	93.13	64.10	
		Synthetic	Zero-shot	63.35	92.40	63.82	
			Fine-tuned	63.17	92.49	63.58	
	ViT-L-14-336	Alt-text	Zero-shot	63.73	92.73	64.31	
			Fine-tuned	64.59	93.35	64.92	
		Synthetic	Zero-shot	63.73	92.73	64.31	
			Fine-tuned	63.33	92.81	63.98	
imagenet1k	ViT-B-32	Alt-text	Zero-shot	63.33	88.81	63.35	
			Fine-tuned	60.33	86.55	60.30	
		Synthetic	Zero-shot	63.33	88.81	63.35	
			Fine-tuned	61.40	87.45	61.37	
	ViT-L-14	Alt-text	Zero-shot	75.54	94.58	75.54	
			Fine-tuned	75.31	94.59	75.33	
		Synthetic	Zero-shot	75.54	94.58	75.54	
			Fine-tuned	75.56	94.63	75.54	
	ViT-L-14-336	Alt-text	Zero-shot	76.57	95.12	76.55	
			Fine-tuned	76.45	95.11	76.42	
		Synthetic	Zero-shot	76.57	95.12	76.55	
			Fine-tuned	76.50	95.12	76.49	

and thematic categorizations, underscores the dataset’s focus on dynamic Earth processes and environmental phenomena, encompassing all the five major Earth spheres: Atmosphere, Hydrosphere, Geosphere, Biosphere, and Cryosphere. The quantitative comparison of synthetic captions with original alt-text highlights the enhancement in textual richness and detail achieved through our annotation pipeline. Synthetic captions exhibit a substantially larger vocabulary, greater length, and more complex sentence structures, offering a far more comprehensive and nuanced textual grounding for the visual content.

Our experiments demonstrate GAIA’s value across vision-language tasks. Fine-tuning CLIP on GAIA improved RS image classification and cross-modal retrieval performance across

all model scales (ViT-B-32, ViT-L-14, ViT-L-14-336), with synthetic captions outperforming alt-text due to their enhanced semantic richness. Gains were most pronounced on EuroSAT (addressing zero-shot CLIP’s RS limitations), while Resisc45 saw more modest improvements—a disparity potentially tied to GAIA’s thematic focus and limited high-resolution imagery. Crucially, GAIA fine-tuning preserved generalizability, maintaining or slightly improving ImageNet1K performance, which underscores positive transfer learning. Similarly, BLIP2 fine-tuned on GAIA achieved substantial gains in captioning metrics and generated more contextually accurate descriptions of Earth events, though limitations like geographic inaccuracies and verbosity persisted. Together, these results highlight

TABLE VI  
CROSS-MODAL RETRIEVAL RESULTS GROUPED BY MODEL AND GAIA CAPTION SCHEME

Model	Captions	Mode	Text-to-Image Recall (%)				Image-to-Text Recall (%)			
			@1	@5	@10	@20	@1	@5	@10	@20
ViT-B-32	Alt-Text	Zero-shot	3.13	9.66	15.08	22.44	2.39	6.77	10.53	15.96
		Fine-tuned	6.37	19.49	29.43	41.52	5.90	19.30	29.06	40.89
	Synthetic	Zero-shot	4.89	13.49	20.03	28.63	4.89	13.96	20.59	29.35
		Fine-tuned	11.02	29.95	42.28	55.80	11.30	30.27	41.70	55.19
ViT-L-14	Alt-Text	Zero-shot	7.92	20.63	30.04	41.34	5.49	13.94	20.64	28.78
		Fine-tuned	11.77	30.59	42.36	56.37	10.60	29.54	41.49	54.87
	Synthetic	Zero-shot	12.69	29.46	39.71	51.38	12.24	29.10	39.20	51.18
		Fine-tuned	19.35	43.47	56.82	70.46	19.21	42.82	56.10	69.25
ViT-L-14-336	Alt-Text	Zero-shot	8.87	23.59	33.57	45.24	6.34	16.34	23.27	32.75
		Fine-tuned	12.43	32.23	44.67	58.77	11.41	31.33	43.24	57.68
	Synthetic	Zero-shot	14.59	33.62	44.66	56.89	15.22	33.68	44.15	55.74
		Fine-tuned	23.03	49.93	62.86	76.20	23.07	48.79	62.20	75.40

TABLE VII  
REMOTE SENSING IMAGE CAPTIONING RESULTS GROUPED BY GAIA CAPTION SCHEME

Target	Mode	Evaluation Metrics (%)				
		BLEU	ROUGE-1	ROUGE-2	ROUGE-L	METEOR
Alt-Text	Zero-shot	0.00	14.05	3.27	13.32	12.35
	Fine-tuned	6.34	26.74	13.30	26.32	26.44
Synthetic	Zero-shot	0.26	22.19	5.77	18.29	9.35
	Fine-tuned	25.76	42.64	19.64	33.91	36.90

GAIA’s dual role: enhancing RS-specific model capabilities through domain-adapted training while retaining foundational visual understanding, with captioning challenges pointing to opportunities for refining annotation pipelines and model architectures.

### B. Future Directions for GAIA and Remote Sensing Vision-Language Models

While the initial experimental results are promising, it is crucial to acknowledge inherent limitations within the scope of this study. Although GAIA represents a substantial advancement in RS dataset scale and annotation quality, its construction is inherently bounded by the availability of publicly accessible RS imagery and associated textual metadata online. Furthermore, the dataset’s thematic emphasis, while advantageous for numerous Earth science applications, may also introduce inherent biases, potentially limiting its generalizability to a broader spectrum of RS tasks beyond event-centric scenarios. It is also crucial to note that the synthetic captions are designed to augment the semantic context provided by the original alt-text, rather than to function as exhaustive, dense annotations capturing every discrete visual element.

To systematically address these identified limitations, our future research trajectory encompasses a series of follow-up investigations. Given the rapid advancements in multi-modal large language models (MLLMs) and the increasing convergence in performance between open-source, open-weight and proprietary models, we strongly believe that it will be feasible to scale our annotation pipeline in a cost-effective manner, enabling us to integrate more data sources.

This expansion will involve both direct web-scraping from the internet and the incorporation of existing web-crawled datasets, such as the filtered RS image-text pairs referenced in Section II-A. Such an approach will enrich GAIA with more generic RS information, moving beyond a predominantly event-oriented sample distribution, and concurrently address the under-representation of complementary data often found in existing datasets such as aerial imagery and very high spatial resolution imagery in general. Moreover, the inclusion of additional dense captions, alongside a dedicated instruction-tuning dataset, is considered essential for the effective training and fine-tuning of state-of-the-art models for the specific challenges of RS vision-language tasks. This is particularly relevant as the preliminary experiments presented herein are limited in scope, primarily evaluating CLIP and BLIP2 models across a subset of common RS applications. Further research is therefore needed to explore the full potential of GAIA across a wider range of VLM architectures and diverse downstream applications within the RS domain. Last but not least, beyond visual and textual data, a critical enhancement for GAIA will be the integration of corresponding RS modalities, such as multi-spectral and Synthetic Aperture Radar (SAR) data. This will offer crucial, complementary information, leading to more comprehensive scene understanding and improved robustness in adverse conditions. Multi-modal VLM approaches have recently seen increased interest [92]–[95] in RS. This dataset expansion is expected to significantly enhance the capabilities of models trained on GAIA and enable the RS community to explore the full potential of our dataset across a wider range of VLM architectures and diverse downstream applications



Fig. 12. GAIA image captioning examples using BLIP2. This figure presents three diverse satellite images featuring diverse Earth Observation scenarios. For each image, we illustrate the corresponding Alt-Text and Synthetic captions along with the zero-shot, alt-text fine-tuned and synthetic fine-tuned predictions, demonstrating the semantic difference between the alt-text and synthetic captions as well as the evolution of captioning capabilities.

within the RS domain.

REFERENCES

[1] Z. Xiong, F. Zhang, Y. Wang, Y. Shi, and X. X. Zhu, "Earthnets: Empowering artificial intelligence for earth observation," *IEEE Geoscience and Remote Sensing Magazine*, 2024.

[2] R. Bommasani, D. A. Hudson, E. Adeli, R. Altman, S. Arora, S. von Arx, M. S. Bernstein, J. Bohg, A. Bosselut, E. Brunskill *et al.*, "On the opportunities and risks of foundation models," *arXiv preprint arXiv:2108.07258*, 2021.

[3] C. Schuhmann, R. Beaumont, R. Vencu, C. Gordon, R. Wightman, M. Cherti, T. Coombes, A. Katta, C. Mullis, M. Wortsman *et al.*, "Laion-5b: An open large-scale dataset for training next generation image-text models," *Advances in Neural Information Processing Systems*, vol. 35, pp. 25 278–25 294, 2022.

[4] S. Y. Gadre, G. Ilharco, A. Fang, J. Hayase, G. Smyrnis, T. Nguyen, R. Marten, M. Wortsman, D. Ghosh, J. Zhang *et al.*, "Datacomp: In search of the next generation of multimodal datasets," *Advances in Neural Information Processing Systems*, vol. 36, 2024.

[5] X. Li, C. Wen, Y. Hu, Z. Yuan, and X. X. Zhu, "Vision-language models in remote sensing: Current progress and future trends," *IEEE Geoscience and Remote Sensing Magazine*, 2024.

[6] M. Czerkawski and A. Francis, "From laion-5b to laion-eo: Filtering billions of images using anchor datasets for satellite image extraction," *arXiv preprint arXiv:2309.15535*, 2023.

[7] B. Qu, X. Li, D. Tao, and X. Lu, "Deep semantic understanding of high resolution remote sensing image," in *2016 International conference on computer, information and telecommunication systems (Cits)*. IEEE, 2016, pp. 1–5.

[8] X. Lu, B. Wang, X. Zheng, and X. Li, "Exploring models and data for remote sensing image caption generation," *IEEE Transactions on Geoscience and Remote Sensing*, vol. 56, no. 4, pp. 2183–2195, 2017.

- [9] Z. Yuan, W. Zhang, K. Fu, X. Li, C. Deng, H. Wang, and X. Sun, "Exploring a fine-grained multiscale method for cross-modal remote sensing image retrieval," *IEEE Transactions on Geoscience and Remote Sensing*, vol. 60, pp. 1–19, 2022.
- [10] Y. Zhan, Z. Xiong, and Y. Yuan, "Rsvg: Exploring data and models for visual grounding on remote sensing data," *IEEE Transactions on Geoscience and Remote Sensing*, vol. 61, pp. 1–13, 2023.
- [11] A. Radford, J. W. Kim, C. Hallacy, A. Ramesh, G. Goh, S. Agarwal, G. Sastry, A. Askell, P. Mishkin, J. Clark *et al.*, "Learning transferable visual models from natural language supervision," in *International conference on machine learning*. PMLR, 2021, pp. 8748–8763.
- [12] H. Liu, C. Li, Q. Wu, and Y. J. Lee, "Visual instruction tuning," *Advances in neural information processing systems*, vol. 36, 2024.
- [13] H. Liu, C. Li, Y. Li, and Y. J. Lee, "Improved baselines with visual instruction tuning," in *Proceedings of the IEEE/CVF Conference on Computer Vision and Pattern Recognition*, 2024, pp. 26 296–26 306.
- [14] A. Panigrahi, S. Verma, M. Terris, and M. Vakalopoulou, "Have foundational models seen satellite images?" in *IGARSS 2023-2023 IEEE International Geoscience and Remote Sensing Symposium*. IEEE, 2023, pp. 4998–5001.
- [15] C. Aybar, L. Yshuaylas, J. Loja, K. Gonzales, F. Herrera, L. Bautista, R. Yali, A. Flores, L. Diaz, N. Cuenca *et al.*, "Cloudsen12, a global dataset for semantic understanding of cloud and cloud shadow in sentinel-2," *Scientific data*, vol. 9, no. 1, p. 782, 2022.
- [16] Z. Wang, R. Prabha, T. Huang, J. Wu, and R. Rajagopal, "Skyscript: A large and semantically diverse vision-language dataset for remote sensing," in *Proceedings of the AAAI Conference on Artificial Intelligence*, vol. 38, no. 6, 2024, pp. 5805–5813.
- [17] Z. Zhang, T. Zhao, Y. Guo, and J. Yin, "Rs5m and georsclip: A large scale vision-language dataset and a large vision-language model for remote sensing," *IEEE Transactions on Geoscience and Remote Sensing*, 2024.
- [18] C. Schuhmann, R. Vencu, R. Beaumont, R. Kaczmarczyk, C. Mullis, A. Katta, T. Coombes, J. Jitsev, and A. Komatsuzaki, "Laion-400m: Open dataset of clip-filtered 400 million image-text pairs," *arXiv preprint arXiv:2111.02114*, 2021.
- [19] C. Schuhmann, A. Köpf, T. Coombes, R. Vencu, B. Trom, and R. Beaumont, "LAION COCO: 600M synthetic captions from LAION2B-EN," 2022.
- [20] M. Byeon, B. Park, H. Kim, S. Lee, W. Baek, and S. Kim, "Coyo-700m: Image-text pair dataset," 2022.
- [21] P. Sharma, N. Ding, S. Goodman, and R. Soricut, "Conceptual captions: A cleaned, hypervised, image alt-text dataset for automatic image captioning," in *Proceedings of the 56th Annual Meeting of the Association for Computational Linguistics (Volume 1: Long Papers)*, 2018, pp. 2556–2565.
- [22] S. Changpinyo, P. Sharma, N. Ding, and R. Soricut, "Conceptual 12m: Pushing web-scale image-text pre-training to recognize long-tail visual concepts," in *Proceedings of the IEEE/CVF conference on computer vision and pattern recognition*, 2021, pp. 3558–3568.
- [23] B. Thomee, D. A. Shamma, G. Friedland, B. Elizalde, K. Ni, D. Poland, D. Borth, and L.-J. Li, "Yfcc100m: The new data in multimedia research," *Communications of the ACM*, vol. 59, no. 2, pp. 64–73, 2016.
- [24] K. Srinivasan, K. Raman, J. Chen, M. Bendersky, and M. Najork, "Wit: Wikipedia-based image text dataset for multimodal multilingual machine learning," in *Proceedings of the 44th international ACM SIGIR conference on research and development in information retrieval*, 2021, pp. 2443–2449.
- [25] K. Desai, G. Kaul, Z. Aysola, and J. Johnson, "Redcaps: Web-curated image-text data created by the people, for the people," *arXiv preprint arXiv:2111.11431*, 2021.
- [26] V. Ordonez, G. Kulkarni, and T. Berg, "Im2text: Describing images using 1 million captioned photographs," *Advances in neural information processing systems*, vol. 24, 2011.
- [27] R. Krishna, Y. Zhu, O. Groth, J. Johnson, K. Hata, J. Kravitz, S. Chen, Y. Kalantidis, L.-J. Li, D. A. Shamma *et al.*, "Visual genome: Connecting language and vision using crowdsourced dense image annotations," *International journal of computer vision*, vol. 123, pp. 32–73, 2017.
- [28] Y. Yang and S. Newsam, "Bag-of-visual-words and spatial extensions for land-use classification," in *Proceedings of the 18th SIGSPATIAL international conference on advances in geographic information systems*, 2010, pp. 270–279.
- [29] Q. Cheng, H. Huang, Y. Xu, Y. Zhou, H. Li, and Z. Wang, "Nwpu-captions dataset and mlca-net for remote sensing image captioning," *IEEE Transactions on Geoscience and Remote Sensing*, vol. 60, pp. 1–19, 2022.
- [30] G. Cheng, J. Han, and X. Lu, "Remote sensing image scene classification: Benchmark and state of the art," *Proceedings of the IEEE*, vol. 105, no. 10, pp. 1865–1883, 2017.
- [31] T. Abdullah, Y. Bazi, M. M. Al Rahhal, M. L. Mekhalif, L. Rangarajan, and M. Zauair, "Textrs: Deep bidirectional triplet network for matching text to remote sensing images," *Remote Sensing*, vol. 12, no. 3, p. 405, 2020.
- [32] G.-S. Xia, J. Hu, F. Hu, B. Shi, X. Bai, Y. Zhong, L. Zhang, and X. Lu, "Aid: A benchmark data set for performance evaluation of aerial scene classification," *IEEE Transactions on Geoscience and Remote Sensing*, vol. 55, no. 7, pp. 3965–3981, 2017.
- [33] W. Zhou, S. Newsam, C. Li, and Z. Shao, "Patternnet: A benchmark dataset for performance evaluation of remote sensing image retrieval," *ISPRS journal of photogrammetry and remote sensing*, vol. 145, pp. 197–209, 2018.
- [34] K. Li, G. Wan, G. Cheng, L. Meng, and J. Han, "Object detection in optical remote sensing images: A survey and a new benchmark," *ISPRS journal of photogrammetry and remote sensing*, vol. 159, pp. 296–307, 2020.
- [35] N. I. Bountos, I. Papoutsis, D. Michail, A. Karavias, P. Elias, and I. Parcharidis, "Hephaestus: A large scale multitask dataset towards insar understanding," in *Proceedings of the IEEE/CVF Conference on Computer Vision and Pattern Recognition (CVPR) Workshops*, June 2022, pp. 1453–1462.
- [36] M. Lazecyk, K. Spaans, P. J. González, Y. Maghsoudi, Y. Morishita, F. Albino, J. Elliott, N. Greenall, E. Hatton, A. Hooper *et al.*, "Licar: An automatic insar tool for measuring and monitoring tectonic and volcanic activity," *Remote Sensing*, vol. 12, no. 15, p. 2430, 2020.
- [37] J. Ge, Y. Zheng, K. Guo, and J. Liang, "Rsteller: Scaling up visual language modeling in remote sensing with rich linguistic semantics from openly available data and large language models," *arXiv preprint arXiv:2408.14744*, 2024.
- [38] G. Sumbul, M. Charfuelan, B. Demir, and V. Markl, "Bigearthnet: A large-scale benchmark archive for remote sensing image understanding," in *IGARSS 2019-2019 IEEE International Geoscience and Remote Sensing Symposium*. IEEE, 2019, pp. 5901–5904.
- [39] G. Sumbul, A. De Wall, T. Kreuziger, F. Marcelino, H. Costa, P. Benevides, M. Caetano, B. Demir, and V. Markl, "Bigearthnet-mm: A large-scale, multimodal, multilabel benchmark archive for remote sensing image classification and retrieval [software and data sets]," *IEEE Geoscience and Remote Sensing Magazine*, vol. 9, no. 3, pp. 174–180, 2021.
- [40] G. Christie, N. Fendley, J. Wilson, and R. Mukherjee, "Functional map of the world," in *Proceedings of the IEEE Conference on Computer Vision and Pattern Recognition*, 2018, pp. 6172–6180.
- [41] Y. Long, G.-S. Xia, S. Li, W. Yang, M. Y. Yang, X. X. Zhu, L. Zhang, and D. Li, "On creating benchmark dataset for aerial image interpretation: Reviews, guidances, and million-aid," *IEEE Journal of selected topics in applied earth observations and remote sensing*, vol. 14, pp. 4205–4230, 2021.
- [42] J. Li, D. Li, S. Savarese, and S. Hoi, "Blip-2: Bootstrapping language-image pre-training with frozen image encoders and large language models," in *International conference on machine learning*. PMLR, 2023, pp. 19 730–19 742.
- [43] Y. Zhao, M. Zhang, B. Yang, Z. Zhang, J. Kang, and J. Gong, "Luojiahog: A hierarchy oriented geo-aware image caption dataset for remote sensing image-text retrieval," *arXiv preprint arXiv:2403.10887*, 2024.
- [44] D. Zhu, J. Chen, X. Shen, X. Li, and M. Elhoseiny, "Minigt-4: Enhancing vision-language understanding with advanced large language models," *arXiv preprint arXiv:2304.10592*, 2023.
- [45] Y. Hu, J. Yuan, C. Wen, X. Lu, and X. Li, "Rsgpt: A remote sensing vision language model and benchmark," *arXiv preprint arXiv:2307.15266*, 2023.
- [46] G.-S. Xia, X. Bai, J. Ding, Z. Zhu, S. Belongie, J. Luo, M. Datcu, M. Pelillo, and L. Zhang, "Dota: A large-scale dataset for object detection in aerial images," in *Proceedings of the IEEE conference on computer vision and pattern recognition*, 2018, pp. 3974–3983.
- [47] Z. Yuan, Z. Xiong, L. Mou, and X. X. Zhu, "Chatearthnet: A global-scale, high-quality image-text dataset for remote sensing," *arXiv preprint arXiv:2402.11325*, 2024.
- [48] D. Muhtar, Z. Li, F. Gu, X. Zhang, and P. Xiao, "Lhrs-bot: Empowering remote sensing with vgi-enhanced large multimodal language model," *arXiv preprint arXiv:2402.02544*, 2024.
- [49] C. Liu, K. Chen, R. Zhao, Z. Zou, and Z. Shi, "Text2earth: Unlocking text-driven remote sensing image generation with a global-scale dataset and a foundation model," *arXiv preprint arXiv:2501.00895*, 2025.

- [50] M. Mendieta, B. Han, X. Shi, Y. Zhu, and C. Chen, "Towards geospatial foundation models via continual pretraining," in *Proceedings of the IEEE/CVF International Conference on Computer Vision*, 2023, pp. 16 806–16 816.
- [51] Y. Wang, N. A. A. Braham, Z. Xiong, C. Liu, C. M. Albrecht, and X. X. Zhu, "Ssl4eo-s12: A large-scale multimodal, multitemporal dataset for self-supervised learning in earth observation [software and data sets]," *IEEE Geoscience and Remote Sensing Magazine*, vol. 11, no. 3, pp. 98–106, 2023.
- [52] G. Ilharco, M. Wortsman, R. Wightman, C. Gordon, N. Carlini, R. Taori, A. Dave, V. Shankar, H. Namkoong, J. Miller, H. Hajishirzi, A. Farhadi, and L. Schmidt, "Openclip," Jul. 2021, if you use this software, please cite it as below. [Online]. Available: <https://doi.org/10.5281/zenodo.5143773>
- [53] M. Cherti, R. Beaumont, R. Wightman, M. Wortsman, G. Ilharco, C. Gordon, C. Schuhmann, L. Schmidt, and J. Jitsev, "Reproducible scaling laws for contrastive language-image learning," in *Proceedings of the IEEE/CVF Conference on Computer Vision and Pattern Recognition*, 2023, pp. 2818–2829.
- [54] A. Fang, A. M. Jose, A. Jain, L. Schmidt, A. Toshev, and V. Shankar, "Data filtering networks," *arXiv preprint arXiv:2309.17425*, 2023.
- [55] H. Xu, S. Xie, X. E. Tan, P.-Y. Huang, R. Howes, V. Sharma, S.-W. Li, G. Ghosh, L. Zettlemoyer, and C. Feichtenhofer, "Demystifying clip data," *arXiv preprint arXiv:2309.16671*, 2023.
- [56] Q. Sun, Y. Fang, L. Wu, X. Wang, and Y. Cao, "Eva-clip: Improved training techniques for clip at scale," *arXiv preprint arXiv:2303.15389*, 2023.
- [57] X. Li, Z. Wang, and C. Xie, "An inverse scaling law for clip training," *arXiv preprint arXiv:2305.07017*, 2023.
- [58] —, "Clipa-v2: Scaling clip training with 81.1% zero-shot imagenet accuracy within a \$10,000 budget; an extra \$4,000 unlocks 81.8% accuracy," *arXiv preprint arXiv:2306.15658*, 2023.
- [59] X. Zhai, B. Mustafa, A. Kolesnikov, and L. Beyer, "Sigmoid loss for language image pre-training," in *2023 IEEE/CVF International Conference on Computer Vision (ICCV)*. Los Alamitos, CA, USA: IEEE Computer Society, oct 2023, pp. 11 941–11 952. [Online]. Available: <https://doi.ieeecomputersociety.org/10.1109/ICCV51070.2023.01100>
- [60] A. Birhane, S. Han, V. Boddeti, S. Luccioni *et al.*, "Into the laion's den: Investigating hate in multimodal datasets," *Advances in Neural Information Processing Systems*, vol. 36, 2024.
- [61] C. Schuhmann, A. Köpf, R. Vencu, T. Coombes, and R. Beaumont, "Laion-coco: 600m synthetic captions from laion2b-en," <https://laion.ai/blog/laion-coco-600m-synthetic-captions-from-laion2b-en/>, 2022, accessed: 2024-12-19.
- [62] L. Fan, D. Krishnan, P. Isola, D. Katabi, and Y. Tian, "Improving clip training with language rewrites," *Advances in Neural Information Processing Systems*, vol. 36, 2024.
- [63] T. Nguyen, S. Y. Gadre, G. Ilharco, S. Oh, and L. Schmidt, "Improving multimodal datasets with image captioning," *Advances in Neural Information Processing Systems*, vol. 36, 2024.
- [64] L. Chen, J. Li, X. Dong, P. Zhang, C. He, J. Wang, F. Zhao, and D. Lin, "Sharegpt4v: Improving large multi-modal models with better captions," in *European Conference on Computer Vision*. Springer, 2025, pp. 370–387.
- [65] Q. Yu, Q. Sun, X. Zhang, Y. Cui, F. Zhang, Y. Cao, X. Wang, and J. Liu, "Capsfusion: Rethinking image-text data at scale," in *Proceedings of the IEEE/CVF Conference on Computer Vision and Pattern Recognition*, 2024, pp. 14 022–14 032.
- [66] H. Xu, P.-Y. Huang, X. E. Tan, C.-F. Yeh, J. Kahn, C. Jou, G. Ghosh, O. Levy, L. Zettlemoyer, W.-t. Yih *et al.*, "Altogether: Image captioning via re-aligning alt-text," *arXiv preprint arXiv:2410.17251*, 2024.
- [67] C. Liu, Z. Wan, H. Wang, Y. Chen, T. Qaiser, C. Jin, F. Yousefi, N. Burlutskiy, and R. Arcucci, "Can medical vision-language pre-training succeed with purely synthetic data?" *arXiv preprint arXiv:2410.13523*, 2024.
- [68] N. Rotstein, D. Bensaïd, S. Brody, R. Ganz, and R. Kimmel, "Fusecap: Leveraging large language models for enriched fused image captions," in *Proceedings of the IEEE/CVF Winter Conference on Applications of Computer Vision*, 2024, pp. 5689–5700.
- [69] S. Sharifzadeh, C. Kaplanis, S. Pathak, D. Kumaran, A. Ilic, J. Mitrovic, C. Blundell, and A. Banino, "Synth<sup>2</sup>: Boosting visual-language models with synthetic captions and image embeddings," *arXiv preprint arXiv:2403.07750*, 2024.
- [70] X. Li, H. Tu, M. Hui, Z. Wang, B. Zhao, J. Xiao, S. Ren, J. Mei, Q. Liu, H. Zheng *et al.*, "What if we recaption billions of web images with llama-3?" *arXiv preprint arXiv:2406.08478*, 2024.
- [71] O. Pelka, S. Koitka, J. Rückert, F. Nensa, and C. M. Friedrich, "Radiology objects in context (roco): a multimodal image dataset," in *Intravascular Imaging and Computer Assisted Stenting and Large-Scale Annotation of Biomedical Data and Expert Label Synthesis: 7th Joint International Workshop, CVII-STENT 2018 and Third International Workshop, LABELS 2018, Held in Conjunction with MICCAI 2018, Granada, Spain, September 16, 2018, Proceedings 3*. Springer, 2018, pp. 180–189.
- [72] S. Subramanian, L. L. Wang, S. Mehta, B. Bogin, M. van Zuylen, S. Parasa, S. Singh, M. Gardner, and H. Hajishirzi, "Medicat: A dataset of medical images, captions, and textual references," *arXiv preprint arXiv:2010.06000*, 2020.
- [73] W. Lin, Z. Zhao, X. Zhang, C. Wu, Y. Zhang, Y. Wang, and W. Xie, "Pmc-clip: Contrastive language-image pre-training using biomedical documents," *arXiv preprint arXiv:2303.07240*, 2023.
- [74] J. Liu, Z. Wang, Q. Ye, D. Chong, P. Zhou, and Y. Hua, "Qilin-med-vl: Towards chinese large vision-language model for general healthcare," *arXiv preprint arXiv:2310.17956*, 2023.
- [75] A. E. Johnson, T. J. Pollard, S. J. Berkowitz, N. R. Greenbaum, M. P. Lungren, C.-y. Deng, R. G. Mark, and S. Horng, "Mimic-cxr, a de-identified publicly available database of chest radiographs with free-text reports," *Scientific data*, vol. 6, no. 1, p. 317, 2019.
- [76] A. Bustos, A. Pertusa, J.-M. Salinas, and M. De La Iglesia-Vaya, "Pachest: A large chest x-ray image dataset with multi-label annotated reports," *Medical image analysis*, vol. 66, p. 101797, 2020.
- [77] M. Li, W. Cai, R. Liu, Y. Weng, X. Zhao, C. Wang, X. Chen, Z. Liu, C. Pan, M. Li *et al.*, "Ffa-ir: Towards an explainable and reliable medical report generation benchmark," in *Thirty-fifth Conference on Neural Information Processing Systems Datasets and Benchmarks Track (Round 2)*, 2021.
- [78] Z. Huang, F. Bianchi, M. Yuksekogonul, T. J. Montine, and J. Zou, "A visual-language foundation model for pathology image analysis using medical twitter," *Nature medicine*, vol. 29, no. 9, pp. 2307–2316, 2023.
- [79] W. O. Ikezogwo, M. S. Seyfioglu, F. Ghezloo, D. S. C. Geva, F. S. Mohammed, P. K. Anand, R. Krishna, and L. Shapiro, "Quilt-1m: One million image-text pairs for histopathology," *arXiv preprint arXiv:2306.11207*, 2023.
- [80] A. Dosovitskiy, L. Beyer, A. Kolesnikov, D. Weissenborn, X. Zhai, T. Unterthiner, M. Dehghani, M. Minderer, G. Heigold, S. Gelly *et al.*, "An image is worth 16x16 words: Transformers for image recognition at scale," *arXiv preprint arXiv:2010.11929*, 2020.
- [81] Y. Li, C. Zhang, G. Yu, Z. Wang, B. Fu, G. Lin, C. Shen, L. Chen, and Y. Wei, "Stablellava: Enhanced visual instruction tuning with synthesized image-dialogue data," *arXiv preprint arXiv:2308.10253*, 2023.
- [82] C. Li, C. Wong, S. Zhang, N. Usuyama, H. Liu, J. Yang, T. Naumann, H. Poon, and J. Gao, "Llava-med: Training a large language-and-vision assistant for biomedicine in one day," *Advances in Neural Information Processing Systems*, vol. 36, 2024.
- [83] K. Papineni, S. Roukos, T. Ward, and W.-J. Zhu, "Bleu: a method for automatic evaluation of machine translation," in *Proceedings of the 40th annual meeting of the Association for Computational Linguistics*, 2002, pp. 311–318.
- [84] C.-Y. Lin, "Rouge: A package for automatic evaluation of summaries," in *Text summarization branches out*, 2004, pp. 74–81.
- [85] S. Banerjee and A. Lavie, "Meteor: An automatic metric for mt evaluation with improved correlation with human judgments," in *Proceedings of the acl workshop on intrinsic and extrinsic evaluation measures for machine translation and/or summarization*, 2005, pp. 65–72.
- [86] G. Niemeyer, "Geohash: a fast, hierarchical, latitude/longitude geocoding system," Weblog post, 2008, accessed: [Date you accessed it, e.g., 2025-01-12]. [Online]. Available: <http://geohash.org/site/tips.html>
- [87] D. P. Kingma and J. Ba, "Adam: A method for stochastic optimization," *arXiv preprint arXiv:1412.6980*, 2014.
- [88] I. Loshchilov and F. Hutter, "Decoupled weight decay regularization," *arXiv preprint arXiv:1711.05101*, 2017.
- [89] M. Andriushchenko, F. D'Angelo, A. Varre, and N. Flammarion, "Why do we need weight decay in modern deep learning?" 2023.
- [90] T. Chen, B. Xu, C. Zhang, and C. Guestrin, "Training deep nets with sublinear memory cost," *arXiv preprint arXiv:1604.06174*, 2016.
- [91] E. J. Hu, Y. Shen, P. Wallis, Z. Allen-Zhu, Y. Li, S. Wang, L. Wang, and W. Chen, "Lora: Low-rank adaptation of large language models," *arXiv preprint arXiv:2106.09685*, 2021.
- [92] A. Zavras, D. Michail, B. Demir, and I. Papoutsis, "Mind the modality gap: Towards a remote sensing vision-language model via cross-modal alignment," *arXiv preprint arXiv:2402.09816*, 2024.

- [93] S. Khanal, S. Sastry, A. Dhakal, and N. Jacobs, "Learning tri-modal embeddings for zero-shot soundscape mapping," in *British Machine Vision Conference (BMVC)*, Nov. 2023.
- [94] K. Klemmer, E. Rolf, C. Robinson, L. Mackey, and M. Rußwurm, "Satclip: Global, general-purpose location embeddings with satellite imagery," *arXiv preprint arXiv:2311.17179*, 2023.
- [95] V. Vivanco Cepeda, G. K. Nayak, and M. Shah, "Geoclip: Clip-inspired alignment between locations and images for effective worldwide geo-localization," *Advances in Neural Information Processing Systems*, vol. 36, 2024.